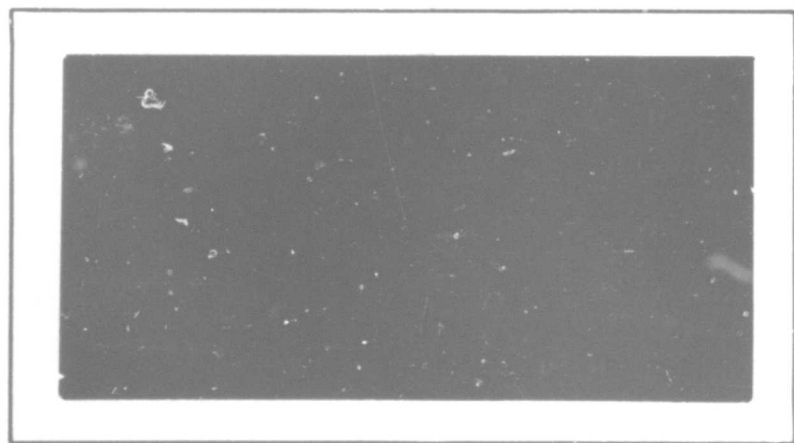


AD857988

AIR FORCE INSTITUTE OF TECHNOLOGY



AIR UNIVERSITY
UNITED STATES AIR FORCE



SCHOOL OF ENGINEERING

WRIGHT-PATTERSON AIR FORCE BASE, OHIO



CONTAINING CONTROLLED FUSION REACTIONS
WITH CROSSED ELECTRIC AND MAGNETIC FIELDS

THESIS

GSP/PH/69-7

Richard D. Franklin
1st Lt USAF

This document is subject to special export controls
and each transmittal to foreign governments or foreign
nationals may be made only with prior approval of the
Dean of Engineering, Air Force Institute of Technology
(AFIT-SE), Wright-Patterson Air Force Base, Ohio 45433

BLANK PAGE

CONTAINING CONTROLLED FUSION REACTIONS
WITH CROSSED ELECTRIC AND MAGNETIC FIELDS

THESIS

Presented to the Faculty of the School of Engineering of
the Air Force Institute of Technology
Air University
in Partial Fulfillment of the
Requirements for the Degree of
Master of Science

by

Richard D. Franklin, B.S.E.E.
1st Lt USAF
Graduate Space Physics
June 1969

Preface

This thesis reports two studies concerned with the feasibility of plasma containment in toroidal magnetic fields. Lt. Col. R. C. Wingerson of the Plasma Physics Research Laboratory of the Aerospace Research Laboratories sponsored this research. Dr. Wingerson's interest in magnetic containment schemes is reflected by the current experimental and theoretical work of the Plasma Physics Research Laboratory, to which this report might hopefully have some application. Much of the theoretical work upon which this thesis is based is Dr. Wingerson's own.

The first part of the study is an investigation of the magnetic field of an infinite system of thin loops of current. The second part develops the equations describing an axisymmetric system of charged particles in crossed electric and magnetic fields.

I would like to thank Dr. Wingerson for his very generously given time and effort. I am also indebted to the Applied Mathematics Research Laboratory and the Digital Computation Division of the Aeronautical Systems Division at Wright-Patterson Air Force Base. My wife has contributed a great deal of encouragement and understanding.

Richard D. Franklin

Contents

	Page
Preface	11
List of Figures	v
List of Tables.	vi
Abstract.	vii
Symbols	viii
I. Introduction	1
Confinement	1
Plasma in Equilibrium	5
II. Magnetic Field of the Displace-Coil Configuration	9
Introduction.	9
Coil Configuration.	10
Objectives of Study	13
Characteristics of B	13
Field Line Paths	13
Methods and Procedures.	14
Ranges of Variables.	14
Bm and RTA	15
Field Line Pattern	16
Results	18
RTA.	18
Bm	21
Uniformity of Bm	21
Field Lines.	21
Summary	24
III. Plasma in Equilibrium.	26
Distribution Function	26
Hydrodynamic Equations.	30
Assumptions.	30
Boltzmann Equation and Moments	31
Maxwell's Equations.	33
Vector Component Equations	33
Normalization.	36
Summary	39

Contents

	Page
IV. Solving the Differential Equations.	41
Introduction	41
Choice of Variables.	42
Initial Conditions	45
Approximate Solution.	51
Origins of Error	55
Numerical Example	57
Change of Variable	59
Numerical Integration.	60
Series Expansions	62
Summary.	65
V. Conclusion.	68
Displaced-Coil Configuration	68
Indirect Solution of Differential Equations.	70
Bibliography	73
Appendix A: Equations of the Displaced-Coil Configuration.	75
Appendix B: The Subroutine Field.	79
Appendix C: The Program Tracer.	90
Appendix D: Collision Force Between Distributions . .	98
Vita	106

GSP/PH/69-7

List of Figures

Figure	Page
1 Schematic of Toroid of Displaced Coils	4
2 Schematic of Infinite System of Thin Loops	12
3 RTA versus Space, Disp, and Alpha.	19
4 dB/dr versus Space, Disp, and Alpha.	20
5 Ten Magnetic Field Lines Traced Over Two Cycles.	22
6 Listing of Field Line Coordinates.	23
7 Cylindrical Coordinate System.	28
8 Flow Diagram of Field.	80
9 Listing of Field	81
10 Flow Diagram of Tracer	91
11 Listing of Tracer.	92

List of Tables

Table	Page
I Normalized Differential Equations	38
II Coefficients of the Polynomial in n	50
III Definitions of Fortran Variables in Field	83
IV Definitions of Fortran Variables in Tracer. . . .	93

Abstract

A toroidal magnetic plasma containment configuration is proposed wherein coils are centered on a closed helix. It is possible to optimize the qualities of the field by adjusting the coil configuration. The equations describing an equilibrium plasma in an axisymmetric system are derived in terms of the particle density distributions, radial and azimuthal drift velocities, and the electric and magnetic field strengths necessary to maintain equilibrium.

Symbols

A_θ	Azimuthal component of magnetic vector potential
a	Radius of current loops in meters
$a_1, b_1,$ c_1, d_1	Coefficients in polynomial expansions of elliptic integrals
α, α	Angle between displacements of neighboring coils
\underline{B}	Magnetic field vector
B_o	Axial magnitude of \underline{B}
B_m	Magnitude of \underline{B}
B_r, B_z	Transverse and axial components of \underline{B} in cylindrical coordinates
B_x, B_y	Transverse components of \underline{B} in cartesian coordinates
C_f	Coefficient of collision force term
c_k, k	Complementary modulus and modulus of elliptic integrals
$disp$	Displacement of coil centers from axis
\underline{E}	Electric field vector
E, K	Complete elliptic integrals of second and first kind, respectively
e	Magnitude of electron charge
err	Maximum relative error in any field line coordinate
$\hat{e}_1, \hat{e}_2, \hat{\theta}$	Orthogonal unit vectors in auxiliary cylindrical coordinate system
\underline{F}	Force on a particle
\underline{F}_c	Average force due to collisions between electrons and ions

F_s	Average force due to acceleration of injected particles
f	Distribution function in phase space
f_0	Arbitrary constant in distribution function
$F(u)$	Particle distribution function of bombarding particles in Coulomb collisions
\mathcal{F}_c	Change in particle momentum per unit time due to collisions
\mathbf{g}	Relative velocity of colliding particles
\mathbf{g}'	Relative velocity of colliding particles after collision
$\hat{\mathbf{g}}, \hat{\mathbf{i}}, \hat{\mathbf{n}}$	Unit vectors of $\mathbf{g} - \mathbf{g}'$
H	Hamiltonian of a particle
h	Increment of independent variable, x
I	Current in a coil in amps
I_e	Integral of collision force between ions and electrons
j	Current density
K	Boltzmann's constant, 1.38×10^{-23} joule/ $^{\circ}\text{K}$
\mathcal{K}	Kinetic energy
M	Reduced mass of electron-ion pair
$m(m_e, m_i)$	Particle mass (electron, ion)
$\hat{\mathbf{m}}$	Unit vector in direction of collision force term
N	Number of iterations in numerical integration scheme
$n(n_e, n_i)$	Particle number density
\mathbf{P}	Pressure tensor
$P(v-v')$	Probability per unit time of change in velocity of a particle from v to v'
P_θ	Azimuthal component of canonical angular momentum

q	Particle charge
R, θ, z	Cylindrical coordinates
r, θ, ϕ	Spherical coordinates
RTA	Ratio of transverse to axial B components in cylindrical coordinates
space	Axial interval between coils
\mathcal{S}	Normalized relative velocity between colliding particles
$T (T_e, T_i)$	Particle temperature
tol	Maximum relative error in B_m
u	Velocity of bombarding particle
\bar{v}	Velocity of center of mass of electron-ion pair
\underline{v}	Particle velocity
$v_r (u_r)$	Electron (ion) average radial velocity
$v_\theta (u_\theta)$	Electron (ion) average azimuthal velocity
v_1, v_2	Transverse velocity components in an auxiliary coordinate system
\underline{v}_0	Original velocity of injected particles
\bar{V}	Ion thermal speed
\bar{v}'	Velocity of particle after Coulomb collision
w	Average azimuthal velocity
X, Y, Z	Cartesian coordinates
x	Initial value of independent variable, x
$y_1^p (y_1^c)$	Predicted (corrected) value of independent variable
y_1	Dependent variable in Taylor series expansion
y_n	Value of independent variable at n th integration step
Z	Ion atomic number

β	Arbitrary constant in particle distribution function
E	Coefficient in electric field equation
ϵ_0	Permittivity in vacuum, 8.85×10^{-12} farad/m
n	10^{20} m $^{-3}$
λ	Arccsin of one half of scattering angle corresponding to cut-off distance for collisions
μ_0	Vacuum permeability, $4\pi \times 10^{-7}$ weber/amp-m
ρ	Difference between ion and electron number densities
ρ_e	Charge density
ρ_o	Normalized difference between electron and ion azimuthal velocities
σ	Collision cross section
τ	Ion cyclotron period
Φ	Error function
ϕ	Electric potential
Ω	Arbitrary constant in particle distribution function
$d\Omega$	Differential solid angle in spherical coordinates
$\omega(\omega_e, \omega_i)$	Rotational frequency

BLANK PAGE

CONTAINING CONTROLLED FUSION REACTIONS
WITH CROSSED ELECTRIC AND MAGNETIC FIELDS

I. Introduction

Dating back to 1944 the possibility of controlled fusion has held the interest of a large segment of the world scientific community. The basic principles of controlled thermonuclear reactions, if not already known, were laid down by scientists at the Los Alamos Scientific Laboratory as early as 1946. Among these were Fermi, Teller, Tuck, and Wilson. Since that time, however, no controlled fusion reactions of extended duration or energy have been possible.

Confinement

One of the major obstacles to controlled fusion is still the need for a method of plasma confinement. Almost all currently proposed methods can be divided into three types of devices: the pinch (Ref 2:22), the magnetic mirror (Ref 2:51), and the torus (Ref 2:33). All of these utilize magnetic fields in attempting to trap the charged particles composing a plasma into helical orbits about field lines. The objective of all methods is to contain the colliding particles long enough for a copious number of nuclear reactions to occur.

A high-temperature plasma is much like an ordinary gas in that it tends to diffuse because of interparticle collisions. Magnetic containment devices are designed to exert containing pressures on the expanding plasma and limit diffusion. It can be shown (Ref 5:275) that the rate of plasma diffusion across a straight, uniform magnetic field is inversely proportional to the square of the magnetic field strength. This is important because it shows that if stable confinement is possible diffusion can be reduced by raising field strength. Thus, if the density of the plasma can be raised high enough, thermonuclear reactions can occur at a self-sustaining rate.

The toroidal magnetic field is attractive for plasma confinement because it presumably does away with the end effects of the pinch and the magnetic mirror. The toroid appears to the plasma as an endless tube. In this type of system the field is generated with current windings around a toroidal shape. The field lines are roughly circles inside the torus. It is easily seen, however, that the field within the torus is stronger at the inside circumference than at the outside of the torus because the windings are closer together.

Several toroidal devices have been proposed and built to correct this non-uniformity. Among them are the Scyllac (Ref 13:543), the Wisconsin (Ref 11:1115), and the most famous, the Stellarator (Ref 2:37).

In 1951 Spitzer proposed a device called the "Stellarator" which introduced a rotation of field lines within a twisted torus. This phenomenon cancelled charged particle drifts transverse to the field. Later he placed helical windings around an ordinary torus which accomplished the same thing.

Part of this thesis is a study of the field of a toroidal device proposed by Lt. Col. R. C. Wingerson of the Plasma Physics Research Laboratory of the Aerospace Research Laboratories. This device is a series of solenoid coils with centers roughly concentric on a circle. The centers of the coils are displaced off the major circumference of a torus by a small distance in such a way as to leave an equal angle between the directions of displacement of successive coils. Fig. 1 is a schematic representation of this system. The parameters of the configuration, such as the number of coils, the spacing between coils, the displacements off axis, and the angle between displacement, are the variables used to manipulate the field.

If only a short segment of the arc of this toroid is considered, the system can be approximated by an infinitely-long straight system of coils. The coils are then plane-parallel.

Chapter II of this paper describes the methods and procedures for the study of the field of this infinite straight system, and it reports the findings. The analysis of the field is directed mainly towards determining the

GSP/PH/69-7

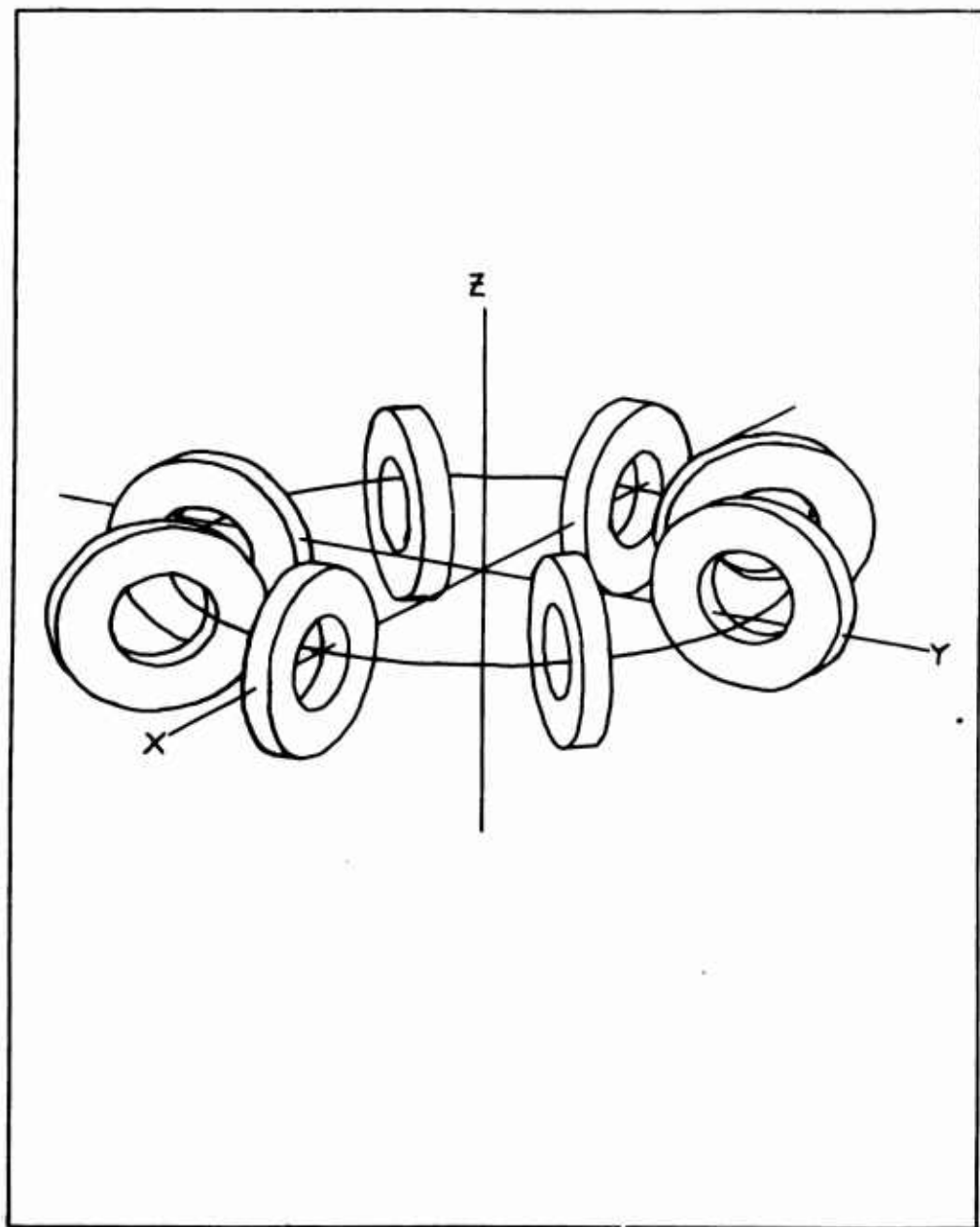


Fig. 1. Schematic of Toroid of Displaced Coils

transverse uniformity of the field strength, the linearity of the field lines and the stellarator-type rotations of the field lines.

The purpose of this study is to determine the feasibility of designing a theoretically useful containment device by adjusting the parameters of the coil configuration. If the characteristics of the field can be controlled by varying the spatial parameters of the coil configuration, we may have a feasible way of designing magnetic fields with very specific properties.

Plasma in Equilibrium

The second part of this study develops the hydrodynamic equations of a system of two types of particles, electrons and positive ions, in equilibrium with an axially directed magnetic field. Only the time-independent case is dealt with. First a generalized distribution function is derived in which particle energy and canonical angular momentum are conserved. The resulting function is essentially Maxwellian, but an azimuthally symmetric rotation of the single distribution is predicted. It is necessary to derive an average volumetric force which arises from collisions between unlike particles in order to account for the interaction of the superimposed distributions.

The steady-state Boltzmann equation is relied upon to provide the hydrodynamic equations for each distribution. Except for the inclusion of a force term describing changes

in the distributions due to collisions, the distributions are treated entirely separately. One of the objectives of the study is to test theoretically the effects on the equilibrium situation of great differences between the electron and ion kinetic temperatures.

Another prime objective of the study is to investigate the feasibility of prescribing radial particle number density profiles by the injection of charged particles. It is assumed that electrons and ions can be separately deposited in the plasma at any radial position and at any time rate desired.

If moments of the Boltzmann equation are taken in cylindrical coordinates, all the variables describing each distribution become averages which are functions of the only independent variable, radius. The two non-zero average velocities are the azimuthal and radial velocities. Density is a third variable describing each distribution. The moments of the Boltzmann equation yield one continuity equation and two momentum transfer equations for each distribution. These six equations are all first order differential equations.

Two of Maxwell's equations apply in the steady-state. Current densities and charge density are finite but are taken as local averages. The magnetic field is assumed axially directed, and its magnitude on axis is to be selected. The electric field is assumed entirely radial in direction, and no external electric field is utilized. In

the cylindrical geometry then Maxwell's equations supply two first order differential equations.

Thus a total of eight simultaneous differential equations are available. They are in terms of the two densities, the pairs of radial and azimuthal average velocities, and the electric and magnetic fields. Thus there are in principle enough differential equations to solve simultaneously for the radial profiles of the distribution variables and the electric and magnetic fields. Since the distribution function is based on an equilibrium system, these profiles should describe an equilibrium plasma.

Procedures are to be developed for studying the effects on such an equilibrium of the injection of particles, and of the imposition of temperatures, and the axial magnetic field. Involved is the development of numerical integration methods for the simultaneous solution of the equations. A careful analysis is made of those characteristics of the hydrodynamic equations which determine the applicability of numerical methods to their solution.

The type of plasma of interest in this study is the high-temperature, high-density thermonuclear ionized gas. It is current opinion that temperatures on the order of $10^8 - 10^9$ °K and particle densities on the order of 10^{16} cm⁻³ are required to sustain fusion reactions in the plasma environment. In Chapter IV some numerical examples are carried out to examine some of the predicted velocities and electric fields which correspond to this type of plasma.

GSP/PH/69-7

Much of the theoretical work leading to the derivation of these equations was done by Dr. Wingerson in unpublished papers. He and the scientists of the Plasma Physics Research Laboratory are at this time actively engaged in the design and testing of axisymmetric plasma systems. It is hoped that the efforts reported in this paper can be applied to the design of experimental plasma containment devices.

II. Magnetic Field of the Displaced-Coil Configuration

Introduction

This chapter is a report of a study on the applicability of a proposed plasma containment device, dubbed the "displaced-coil configuration." The major objective of the study was to determine how the characteristics of the field of a device similar to the system of coils shown in Fig. 1 depend on the geometric arrangement of the separate coils. Some of these important characteristics are mentioned in Chapter I; of interest are the gradients of field strength through the field, the direction of the field, and the stellarator rotations of field lines in the field. It was not the objective of the study to determine what field characteristics are necessary or desirable for plasma containment. Nor was the objective to design a magnetic field using the displaced-coil configuration. This study was made to ascertain the feasibility of controlling the major characteristics of a toroidal magnetic field by varying the geometric parameters of the displaced-coil configuration.

First, the geometry of a straight coil configuration which approximates the configuration of Fig. 1 is defined. Notation of variables is established. An orthogonal coordinate system is also defined relative to the coil system.

The equations for the vector components of \underline{B} are derived, and computer programs are described which calculate the magnitude and direction of \underline{B} . Procedures are

developed to systematically investigate field variables as functions of field position and the geometric parameters.

The method of generating mathematically the field lines of the magnetic field is explained. Two characteristics of interest in the pattern of field lines are identified, and the procedures for studying each are explained.

The section covering results reports the variations of the quantities of interest through the field, and their functional relationships to the geometric parameters. The feasibility of designing fields with very particular characteristics is ascertained.

Coil Configuration

Let us consider as an approximation to the torus of real multiple-turn coils an infinite straight system of thin, single-loop coils. The approximation is valid if only a small segment of arc of the torus of solenoids is considered.

The magnetic field of a single loop of current is very similar to that of a finite solenoid. The strength of the \underline{B} field varies similarly in either as a function of position, and the shapes of the fields of the two are characteristically the same.

The equations of the transverse and axial components of \underline{B} for an infinitely-thin loop of current are presented in Appendix A. Techniques are derived there for computing numerical values for these components.

Fig. 2 is a schematic representation of the scheme for constructing the infinite straight system of coils. The axial interval between coils is designated "space." The displacement of the coil centers off the Z axis is "disp." These equal displacements are made such that there is a constant angle "alpha" between the directions of disp of neighboring coils. The arbitrary convention is made that the sign of alpha is positive as measured from one coil center to the next when proceeding from coil to coil in the positive axial direction. The radius of all coils is "a."

The result of these manipulations is a configuration of plane-parallel loops whose centers lie on a uniform helix. The pitch length of the helix is the product of space and alpha, and its radius is disp. The axis of the helix is chosen as the Z axis of an orthogonal coordinate system. The X axis of the system is arbitrarily located through the center of one of the coils.

Let the radii of the coils be normalized to unity, and let all distances henceforth be measured in units of coil radius. Choose the currents in the coils to be equal, in the same direction, and of magnitude such that

$$\frac{\mu_0 I}{2\pi} = 1 \quad (1)$$

This concludes the definition of the displaced-coil configuration. Its geometric parameters are space, disp, and alpha. This chapter is primarily concerned with the dependence of the magnetic field on these three variables.

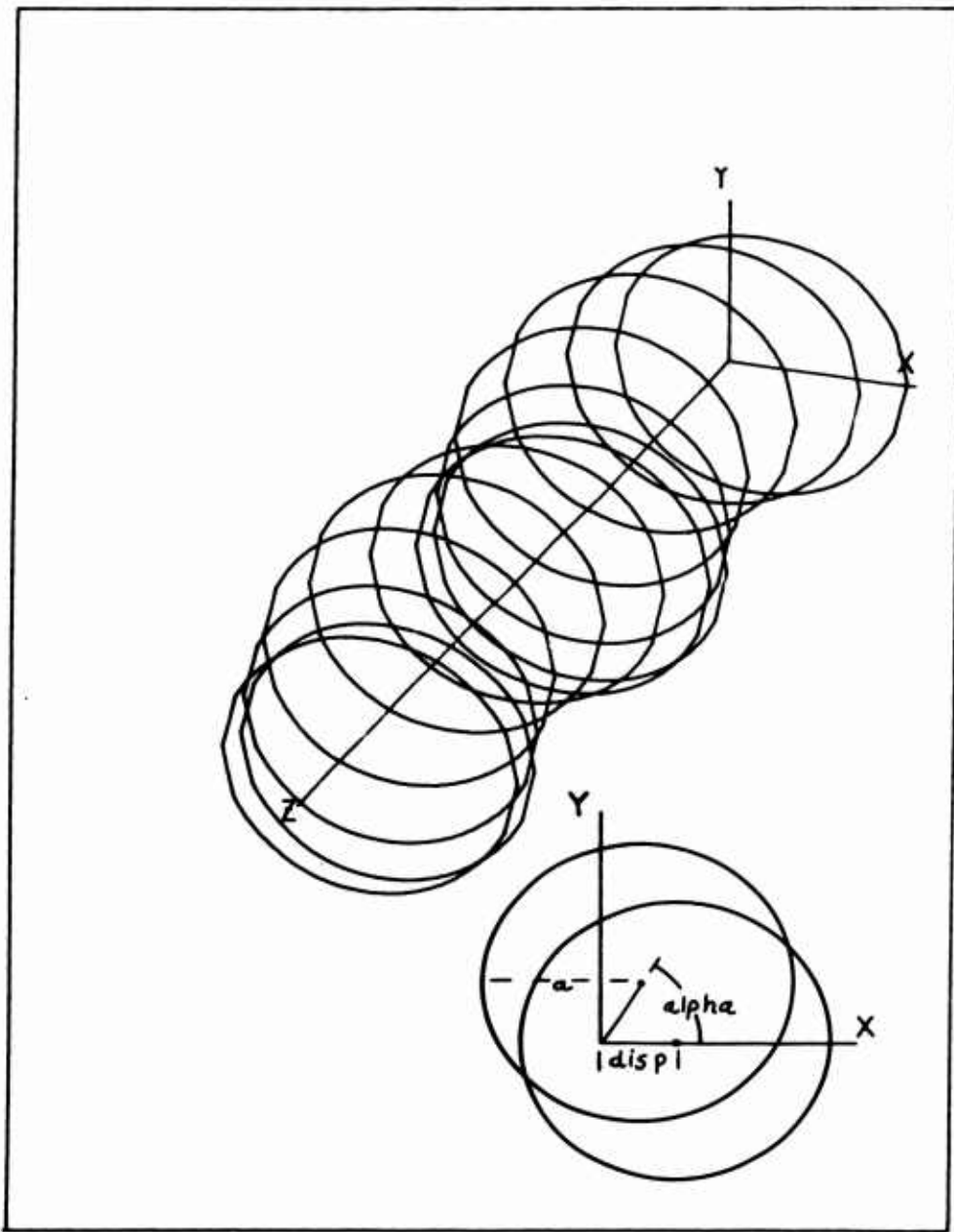


Fig. 2. Schematic of Infinite System of Thin Loops

Objectives of Study

This section describes more fully the areas to be investigated in this study. It also attempts to supplement Chapter I in its justification of the study.

Characteristics of B. Again, the properties of B most critical to containment feasibility are uniformity of strength and the ratio of transverse to axial component strengths. This study attempts first to discover in general the orders of magnitude of these properties. Then relations between them and the three configuration parameters are sought. The variations of the two properties, as functions of both the radius out from the axis and position along the axis, are also investigated.

Field Line Paths. The magnetic field lines surrounding a single thin loop are closed loops in planes perpendicular to the plane of the loop. Field strengths vary along the paths of these lines, but the magnitudes are symmetric about the plane of the loop.

When many single loops are arranged with their centers on a helix the field lines of the field can no longer be planar. The field is expected to exhibit a helical twist in the region inside all coils.

Questions immediately come to mind. Do the field lines encircle the axis of the system as does the helix described by the coil centers, or do they remain in the same quadrant of the system? Do subharmonics of this field line twist exist such that the entire field line pattern

rotates as a solid body? No matter how either of these rotations appear their frequencies and the radii of the resulting helices should be determined.

Methods and Procedures

This section outlines the computational methods and procedures employed in studying the magnetic field. Appendices are used to support this explanation. Appendix A is the derivation of the numerical approximations for the transverse and axial vector components of \mathbf{B} . Appendix B describes a computer subroutine called "Field" which computes the direction cosines and strength of \mathbf{B} at any given point in the field. The program "Tracer" is explained in Appendix C; it is designed to integrate the paths of the field lines.

Ranges of Variables. The volume of interest in the magnetic field, and the ranges over which the geometric parameters are to be studied need specification. Because of the undesirable behavior of the field variables near the conductors, the volume over which the field is expected to be at all well-behaved is limited to be entirely within all conductors. The size of disp obviously determines the size of the volume satisfying this condition.

The ranges of the geometric parameters to be considered in this study are as follows:

space: 0.1 — 1.0

disp: 0. — 0.2

alpha: 0 — 180 degrees

Limits are imposed on space and disp only for definiteness, and are not meant to be exclusive. They can be expanded if they do not seem to include all the interesting cases. By symmetry the range of alpha covers also the cases for alpha greater than 180 degrees. The above intervals are subdivided sufficiently to reveal the important functional relationships.

Bm and RTA. Let "Bm" refer to the magnitude of B. Appendix A presents the equations for the axial (Bz) component and the total component transverse to the axis (Br). Let "RTA" stand for the ratio of Br and Bz. Field is a subroutine which can deliver Bm and RTA at any location.

The procedure is to compute both these terms for any given set of space, disp, and alpha at several different radii within all loops and also at points along the axis between any two loops. The computations for varying radius are conducted halfway between two coils to minimize anomalies due to nearby conductors.

The analysis of results consists first of finding how RTA varies with space, disp, alpha, radius from the axis, and position along the axis. Then the rates of change of Bm with radius and axial position are determined as generalized functions. Finally, these rates of change, $\partial Bm/\partial r$ and $\partial Bm/\partial z$, are investigated as functions of space, disp, and alpha. Since the normalized Bm is a strong function of space, it is necessary to calculate $\partial Bm/\partial r$ and $\partial Bm/\partial z$ as relative rates of change.

Field Line Pattern. We have mentioned that the following two phenomena are probably of interest: the helical twist of the lines caused by the helical coil configuration, and the possible slow rotations of the entire field line pattern about the axis. Let us call the helical twist a first order occurrence. This twist is studied as a function of radial position in the field and of the coil geometry.

Field lines are traced over one repetition or cycle of coil displacement. The tracings are begun from points at various radii in the plane of an arbitrary coil.

A convenient measure of the resulting helices is the helical radius. It is expected that the pitch length of the first order twist is the same as that of the coil pattern. That is, the pitch length of the lines should be the same as that of the coil center helix. This must be verified, however.

It is necessary to determine if the second type of rotation is important to the shape of the field. These rotational drifts become evident only over several cycles of the first order twist. Therefore, a few lines beginning at different radii are traced over one hundred first order cycles for several sets of space, disp, and alpha. If the frequency of the rotation of any line around the axis is such that the axis is encircled in less than one hundred cycles, the second order rotation may be important. A more detailed analysis of the frequencies of these rotations is then to be undertaken.

The field lines are generated by successively integrating, point by point, the direction cosines of B over incremental distances. Appendix C describes and gives operating instructions for a program which integrates lines, beginning at selected X-Y coordinates, over selected distances.

The program supplies a record of the three coordinates of points along the field line. It is also written to be amenable to plotting subroutines so that the lines can be traced in machine drawings.

The diameters of the first order helices are easily calculable from the printed records of the X and Y coordinates of a line. We need merely subtract, say, the minimum X coordinate from the maximum. Tracer supplies these coordinates to four places.

The pitch length of the lines is the same as that of the coil-center helix if the field lines cross the planes of concentric coils at the same X and Y coordinates. Appendix C details the maximum errors in these coordinates which can arise out of the numerical integration methods utilized.

To measure the frequencies of the drifts, the numerical listing of point coordinates is studied to find the differences in both the X and Y coordinates of a line as it passes through the planes of coils one hundred first order cycles apart. The resulting differences give a good average measure of the magnitude and direction of the drift of a

particular line.

Results

This section is a report of how the characteristics of the field of the displaced-coil configuration vary with space, disp, and alpha. The dependence of RTA and the uniformity of B_m on these parameters is presented graphically in Figs. 3 and 4. These curves quantitatively depict RTA and the relative gradient with radius of B_m on axis, halfway between any two coils. However, curves were drawn for other locations in the field, and their shapes are very similar to the curves in Figs. 3 and 4. The general dependence of RTA and B_m on position in the field is qualitatively described below. Also, sample computations of RTA and dB/dr for values of space, disp, and alpha not included in the ranges previously set down indicated no unexpected behavior.

RTA. Fig. 3 contains graphs of RTA on axis as a function of each of the configuration parameters alone, holding the other two parameters fixed. RTA is a strong function of all three geometric parameters and of radial position in the field. The almost linear function of RTA with disp is predictable. Increasing disp accentuates the helical twist of the field lines, and hence the transverse components of \mathbf{B} , of which RTA is a measure. RTA increases exponentially with radius from the axis. The rate of increase with radius depends on the specific combination of space, disp, and alpha.

GSP/PH/69-7

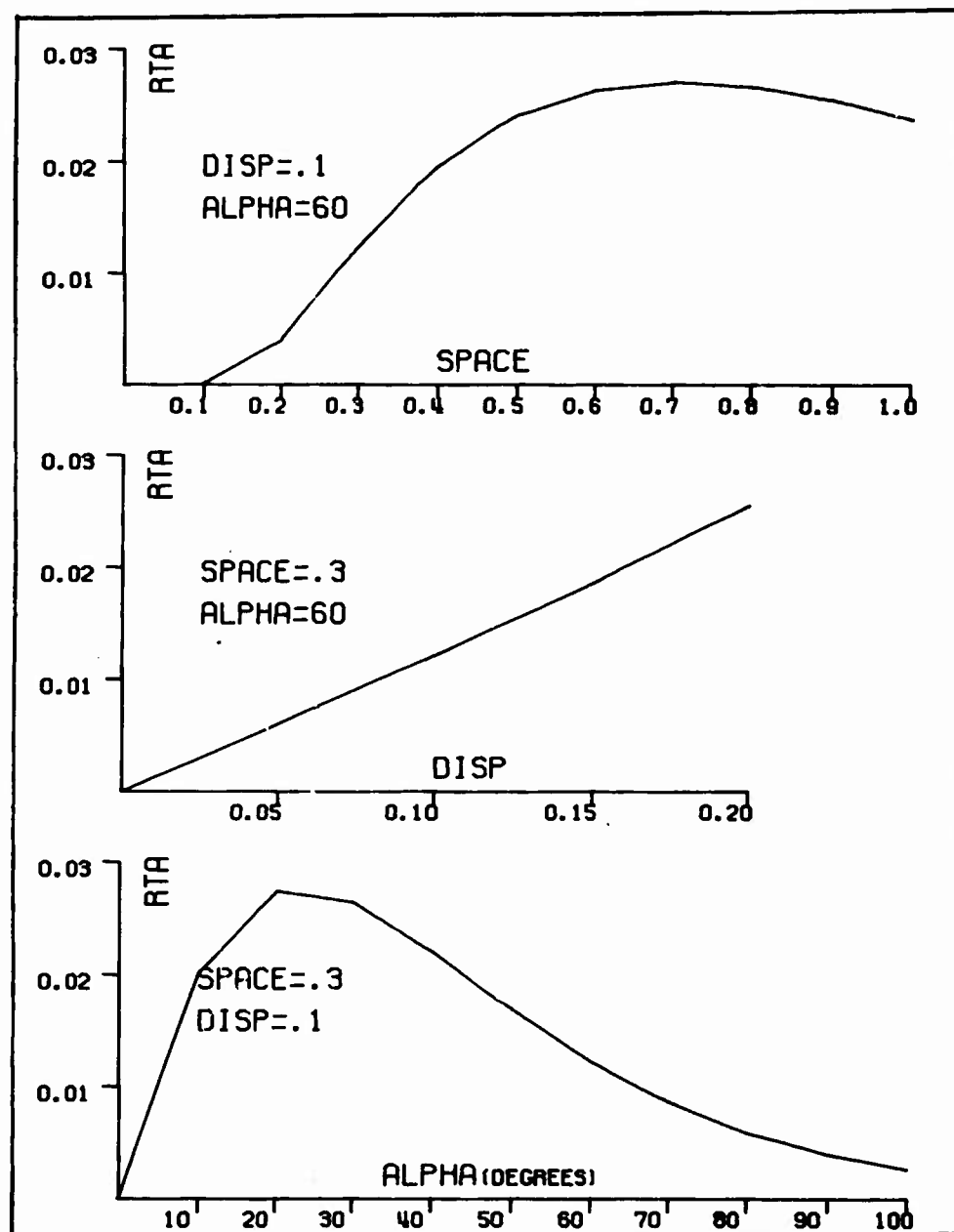


Fig. 3. RTA versus Space, Disp, and Alpha

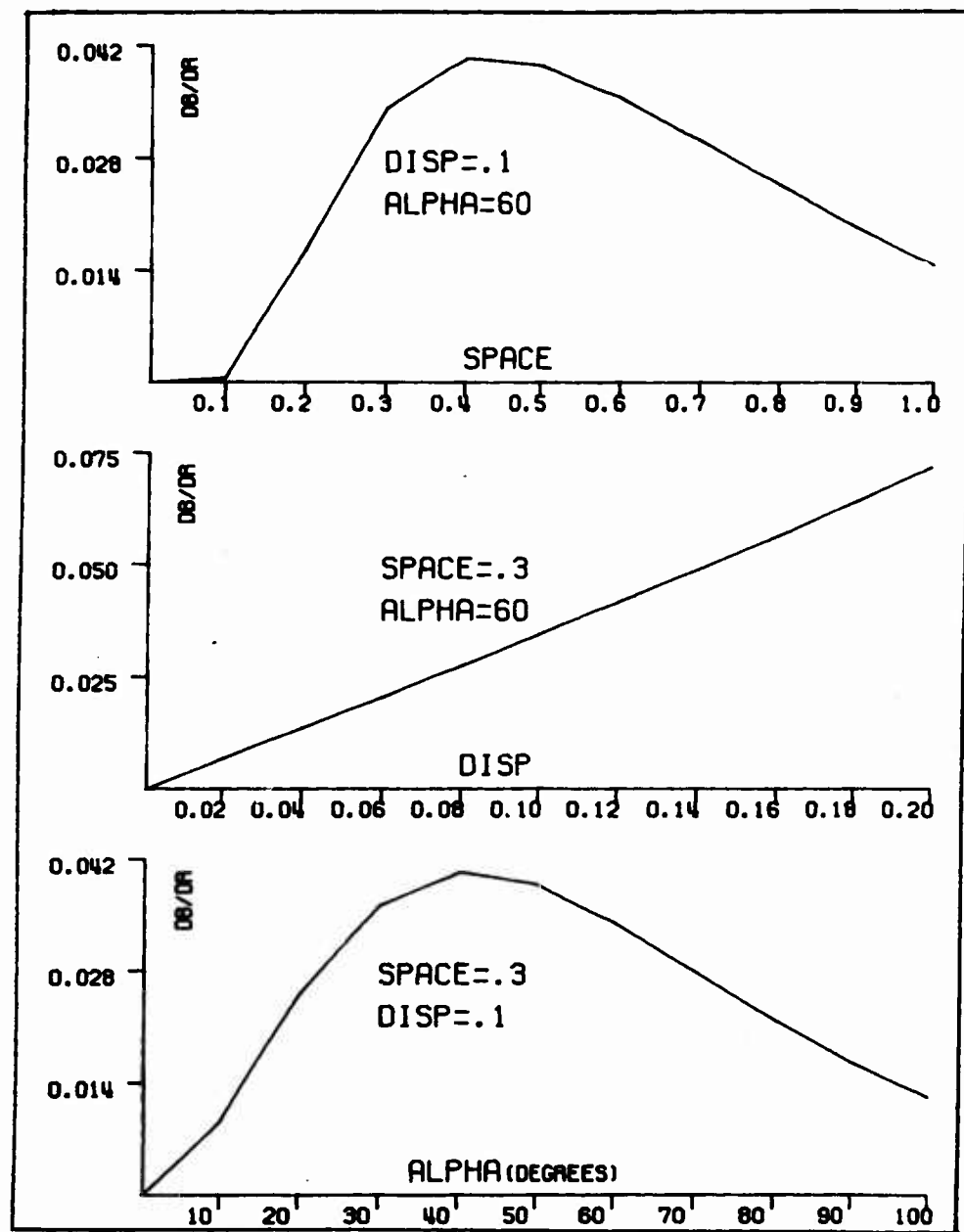


Fig. 4. dB/dr versus Space, Disp, and Alpha

B_m. The mean magnitude B is inversely proportional to space, and is not strongly dependent on disp and alpha. The dependence on space is expected since in general the magnetic field of a coil varies inversely with distance from the center of the coil.

Uniformity of B_m. Consider first the relative quantity dB/dr on axis as a function of space, disp, and alpha as depicted in Fig. 4. Note that the curves of dB/dr are very much like the RTA curves. B_m does not vary azimuthally near the axis, that is, well within all the coils. With increasing radius, as the coils themselves are approached, the field is dominated by the nearest coils. It is difficult to describe in general the field near the coils. B_m is quite uniform along the axis. As a quantitative example, B_m varies along the axis by less than three percent for space equal to unity.

Field Lines. Fig. 5 shows the paths of ten field lines traced over two cycles of coil displacement. Fig. 6 is a listing of coordinates along the line nearest the axis for two cycles. The coil configuration for these lines is defined as follows:

```
space = .6
disp  = .2
alpha = 60°
```

The pitch length of the line twist is the same as that of the coil center helix. The radius of the helical line on axis is .07. The radii of the helices described by

GSP/PH/69-7

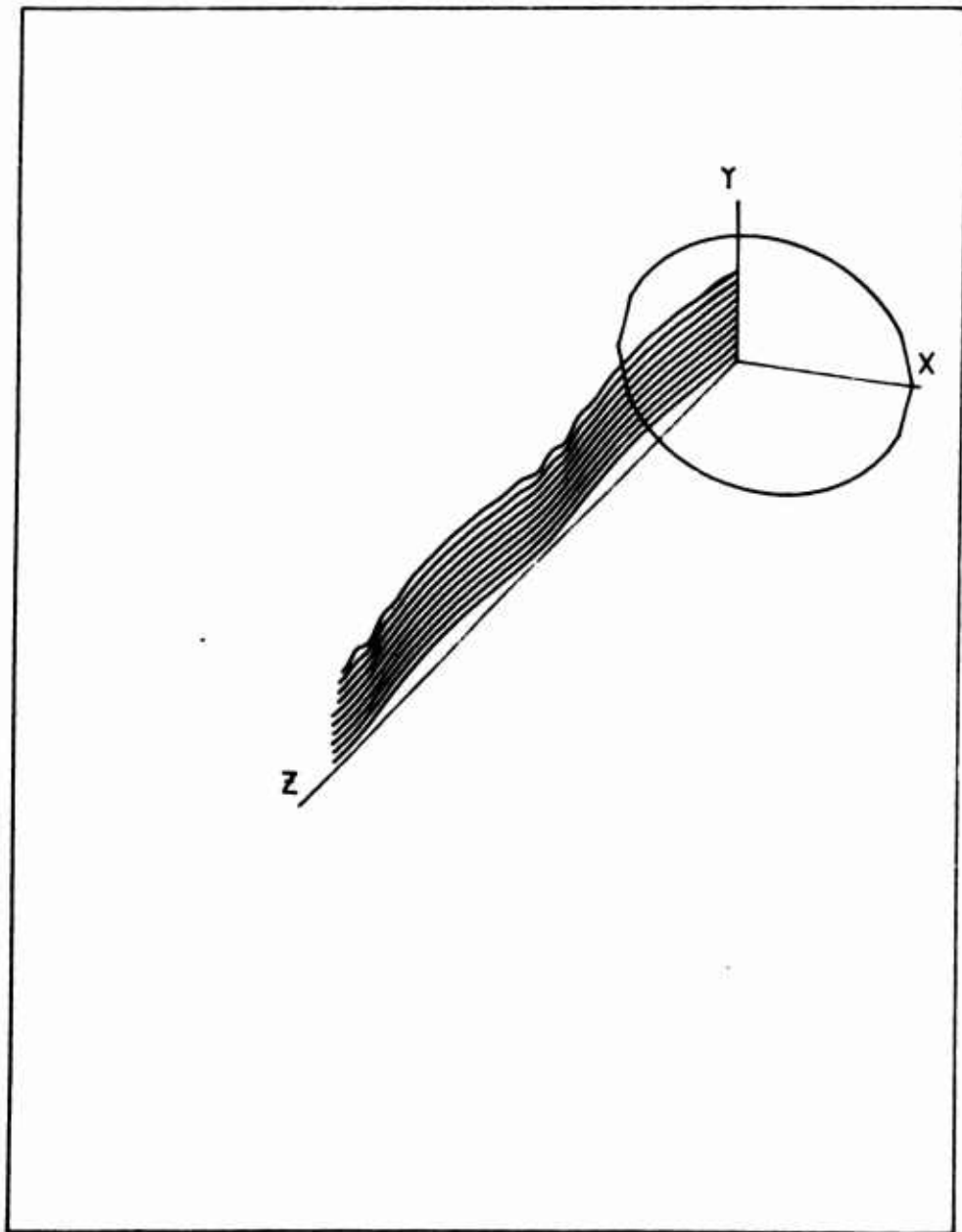


Fig. 5. Ten Magnetic Field Lines Traced Over Two Cycles

SPACE BETWEEN COILS 3.000
 DISPLACEMENT OF COIL CENTER 0.20
 ANGLE BETWEEN CENTERS 60.0 DEGREES

POINT COORDINATES		
X	Y	Z
0.0000	0.0700	0.
0.0036	0.0815	0.1996
0.0037	0.0940	0.2992
-0.0005	0.1055	0.5989
-0.0084	0.1147	0.7985
-0.0191	0.1209	0.9981
-0.0311	0.1231	1.1977
-0.0431	0.1216	1.3973
-0.0537	0.1149	1.5970
-0.0617	0.1057	1.7966
-0.0659	0.0943	1.9962
-0.0661	0.0819	2.1956
-0.0623	0.0703	2.3955
-0.0545	0.0609	2.5951
-0.0439	0.0545	2.7947
-0.0328	0.0520	2.9943
-0.0224	0.0541	3.1939
-0.0194	0.0603	3.3936
-0.0014	0.0594	3.5932
0.0027	0.0698	3.7928
0.0120	0.0933	3.9924
0.0214	0.1048	4.1920
0.0392	0.1142	4.3917
0.0219	0.1204	4.5913
0.0318	0.1228	4.7909
0.0432	0.1258	4.9905
0.0543	0.1149	5.1902
0.0625	0.1058	5.3858
0.0669	0.0945	5.5894
0.0673	0.0821	5.7890
0.0635	0.0705	5.9887
0.0559	0.0610	6.1883
0.0454	0.0545	6.3879
0.0336	0.0518	6.5875
0.0217	0.0538	6.7872
0.0109	0.0598	6.9868
0.0027	0.0689	7.1864

Fig. 6. Listing of Field Line Coordinates

lines farther off the axis increase exponentially from this value. This behavior explains the dependence of RTA on radius from the axis. The pattern of the first order twist shown in Fig. 5 is symmetric about the axis.

From Fig. 5 it appears that the field lines do not tend to rotate about the Z axis of the system. Actually there is a slight drift of these lines about the axis. Selected lines were integrated over one hundred first order cycles for various combinations of space, disp, and alpha. The transverse coordinates of the lines did not return to their starting values after each first order revolution. The indicated drifts over one hundred first order cycles were extrapolated to compute how many first order cycles would be required to encircle the Z axis and return to the transverse starting coordinates. On the average these extrapolations indicated that it takes about 100,000 first order cycles for the field lines to encircle the axis.

Summary

We have investigated the magnetic field of the displaced-coil configuration. Two characteristics, the uniformity of field magnitude and the ratio of transverse to axial field components, have been analyzed as functions of space, disp, alpha, and location within the field. The pattern of field lines has been ascertained.

The qualities of a magnetic field which are important to plasma containment seem to be controllable by adjustment of the coil configuration. The field lines are helices,

and the entire field seems to rotate about the central axis.

Note that the displaced-coil configuration does not depend on any particular solenoidal windings as far as shape or size are concerned. Standard solenoids, commercially available, could be used as long as the minimum required field strengths could be attained. Field design is accomplished solely through the geometric arrangement of the coils. Thus the necessity of designing and constructing special windings is eliminated. Many different configurations could be experimentally tested cheaply and conveniently.

It is mentioned in Chapter I that stellarator-type revolutions of the field lines can be useful in cancelling the drifts of charged particles in a toroidal magnetic field. Although this study concentrates on an infinite straight coil configuration, it was demonstrated that rotation of the field lines does take place. The toroidal coil configuration from which the straight system is derived would also cause the field lines to rotate. Hence the advantages of the stellarator would be available without the additional stellarator windings.

III. Plasma in Equilibrium

In this chapter the steady-state hydrodynamic equations of a plasma in equilibrium in an axisymmetric system are derived. The distribution function for a system of like particles is first derived from Liouville's equation. The distribution function is applied separately for ions and electrons. The hydrodynamic equations for each distribution are found as moments of the Boltzmann equation. Two of Maxwell's equations can be applied to the axisymmetric system. The result is a system of eight simultaneous, first order differential equations in terms of eight unknown variables.

Distribution Function

From Liouville's theorem (Ref 7:56) the most general equilibrium distribution for a system of like particles is a function only of the Hamiltonian constants of motion. In an axisymmetric system two appropriate dynamical constants are the Hamiltonian and the canonical angular momentum.

$$H = \frac{1}{2}mv^2 + q\phi \quad (2)$$

$$P_e = mr\omega + q\mathbf{r}\mathbf{A}_e \quad (3)$$

Then a distribution function which is consistent with the conservation of H and P_θ is

$$f = f_0 \exp -\beta [H - \Omega P_\theta]$$

$$= f_0 \exp -\beta \left[\frac{1}{2}mv^2 + q\phi - \Omega mr\omega - \Omega qrA_\theta \right] \quad (4)$$

where f_0 , β , and Ω are arbitrary constants. In principle all variables of the system of particles obeying this distribution can be found as moments of the function. However, it is convenient to transform to another coordinate system before taking moments.

Let a coordinate system be chosen in which the orthogonal unit vectors are $\hat{\mathbf{e}}_1$, $\hat{\mathbf{e}}_2$, and $\hat{\mathbf{e}}_\theta$, such that

$$\underline{\mathbf{B}} = B \hat{\mathbf{e}}_\theta \quad (5)$$

and

$$\hat{\mathbf{e}}_2 = \hat{\mathbf{e}}_\theta \times \hat{\mathbf{e}}_1 \quad (6)$$

The new system is illustrated in Fig. 7.

Let us make the convention that the $\hat{\mathbf{e}}_\theta$ direction always coincides with the azimuthal direction relative to the original cylindrical coordinate system. Then the product $(r\omega)$ in Eq. (3) is azimuthal velocity, and is in the $\hat{\mathbf{e}}_\theta$ direction. The other two components of total particle velocity can be called v_1 and v_2 . Thus

$$v^2 = v_1^2 + v_2^2 + [r\omega]^2 \quad (7)$$

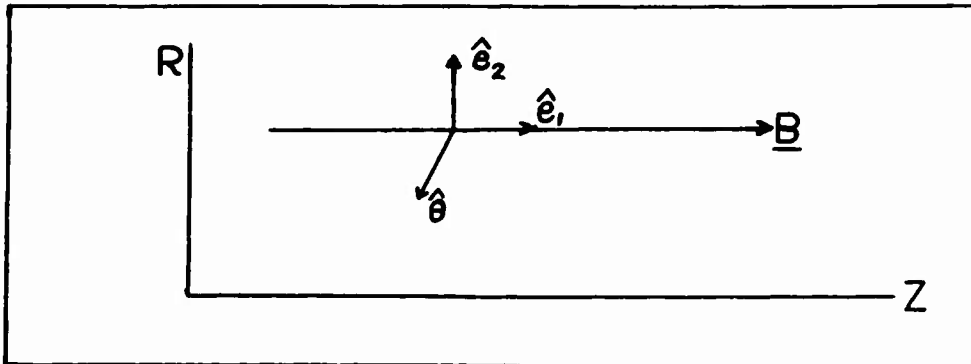


Fig. 7. Cylindrical Coordinate System

The distribution can now be written

$$f = f_0 \exp -\beta [q[\phi - r\Omega A_\theta] + \frac{1}{2}m[v_r^2 + v_z^2 + (r\omega)^2] - r\Omega mr\omega] \quad (8)$$

If we add and subtract the quantity $\frac{1}{2}m(r\Omega)^2$ in the exponent, the terms of f can be rearranged:

$$f = f_0 \exp -\beta [q[\phi - r\Omega A_\theta] + \frac{1}{2}m[v_r^2 + v_z^2] - \frac{1}{2}m[r\Omega]^2 + \frac{1}{2}m[r\omega - r\Omega]^2] \quad (9)$$

Certain moments can now be conveniently calculated.

Particle density is

$$n = \int f d\mathbf{v} \quad (10)$$

where each component of velocity must be integrated from minus infinity to plus infinity.

$$n = f \left(\frac{2\pi}{\beta m} \right)^{3/2} \exp -\beta \left[q[\phi - r\Omega A_0] - \frac{1}{2} m [r\Omega]^2 \right] \quad (11)$$

(Ref 8:284). Define the average azimuthal particle velocity as w .

$$w = \frac{1}{n} \int [rw] f dy = r\Omega \quad (12)$$

Average particle kinetic energy is

$$K = \frac{1}{2} \frac{m}{n} \int v^2 f dv = \frac{3}{2\beta} + \frac{1}{2} m [r\Omega]^2 \quad (13)$$

These last three equations suggest the following conclusions:

1. The density distribution is not necessarily constant with radius in the azimuthal system.
2. The plasma exhibits rotation as a solid at an angular frequency Ω .
3. Particle energy is partitioned between the kinetic energy associated with random velocities and the kinetic energy of an average rotation. If $\beta = 1/kt$, the distribution behaves like a Maxwellian distribution with a drift velocity of $(r\Omega)$ superimposed.

The distribution function derived above describes a system of like particles in an axial magnetic field. It

implicitly accounts for interactions between like particles. The derivation is not valid if different types of particles are considered together because it does not account for collisions between unlike particles. However, a real plasma composed of weakly interacting electrons and ions can be described by applying Eq (9) separately for each distribution if the interaction between them can be expressed. The two distributions can be approximately connected via an inter-particle collision force. Appendix D derives the expression for such a force. The interaction force can be expressed as an average force arising from collisions between electrons and ions. The force is proportional to the product of the two local densities and the difference between the two average rates of rotation. The force then can be thought of as an average drag between two distributions rotating at different frequencies.

Hydrodynamic Equations

This section outlines the derivation of the equations describing a system of electrons and ions nearly in equilibrium. The relations employed are the Boltzmann phase-space equation and Maxwell's equations. Mks units are used throughout.

Assumptions. The assumption of an axially directed magnetic field has already been made. Assume also a purely radial electric field. It was mentioned in Chapter I that we wish to investigate the effects of artificially inserting ions and electrons into the plasma. Assume, therefore, that

particles may be inserted anywhere within the plasma at any time rate desired. For instance, ions and electrons may be deposited separately or together, according to some continuous radial distribution or perhaps only within a cylindrical band of some Δr in the system.

Boltzmann's Equation and Moments. The steady-state Boltzmann relation for a system of like particles obeying the distribution function of f is

$$\underline{v} \cdot \nabla f + \frac{\underline{F}}{m} \cdot \nabla_v f = \frac{\partial f}{\partial t} \Big|_{\text{coll}} \quad (14)$$

where

$$f = f(r, \underline{v}) \quad (15)$$

$$\underline{F} = \underline{F}(r, \underline{v}) \quad (16)$$

(Ref 16:155). \underline{F} is used here as the sum of all applied forces which may be described as averages. $\partial f / \partial t$ accounts for processes such as ionization or recombination, charge exchange, or creation of particles.

\underline{F} is composed of the following:

$$\underline{F} = q \left[\underline{E} + \underline{v} \times \underline{B} \right] + \underline{F}_s + \underline{F}_c/n \quad (17)$$

The first term is simply the classical Lorentz force on a charged particle of velocity \underline{v} . \underline{F}_c is the average volumetric force due to collisions between unlike particles. It is divided by density, n , in order to reduce it to a particulate term.

F_s is the average force per particle necessary to accelerate newly created particles from their original input velocities to the local average velocity of like particles in the plasma. The process of acceleration is assumed to be by elastic collisions with like particles only. This assumption is justified by the very small degree of energy transfer in collisions between electrons and ions. Electron-ion collisions tend mainly to randomize the electron velocities; ion velocities are not appreciably changed in such collisions.

Define S as the time rate of creation of particle density at any given point. Consistent with this definition

$$\underline{F}_s = -m [\underline{v} - \underline{v}_o] \frac{S}{n} \quad (18)$$

where v is local velocity and v_o is the original velocity of the new particle. The minus sign on the force conforms to the use of F_s as a force applied to the distribution. Let us assume henceforth that new particles are input at zero velocity. This is not a dangerous assumption in that we must assume that we may control the input velocity anyway. It will be seen that v_o can be reinstated at a finite value at a later point in the derivation with little difficulty.

Macroscopic equations of a plasma are derived as moments of the Boltzmann equation. The first moment is the continuity relation.

$$\nabla \cdot [v n] = S \quad (19)$$

The second moment describes momentum transfer per particle. In steady-state:

$$m [v \cdot \nabla] v = -\frac{\nabla \cdot \overleftrightarrow{P}}{n} + \underline{E} \quad (20)$$

(Ref 18:161), where \overleftrightarrow{P} is the pressure tensor.

If a Maxwellian distribution is assumed locally for each distribution, the pressure tensor is a diagonal with equal terms (Ref 19:24).

$$P = n K T \quad (21)$$

The most important assumption implicit in the use of this term is that the pressure on a single distribution is due only to random motion of particles and collisions between like particles.

Maxwell's Equations. Under the assumptions in force two of Maxwell's equations supply useful relations.

$$\nabla \times \underline{B} = \underline{j} \quad (22)$$

$$\nabla \cdot \underline{E} = \rho/\epsilon \quad (23)$$

where ρ_e is charge density and \underline{j} is current density.

Vector Component Equations. In cylindrical coordinates the continuity relation is simply a scalar equation.

$$\frac{1}{r} \frac{d[r n v_r]}{dr} = S \quad (24)$$

where v_r is the average radial drift velocity of particles out of the system. Note that only partial derivatives with respect to r are non-zero in an axisymmetric system.

The momentum transfer vector equation supplies two vector component equations. The radial vector component equation is

$$m \left[v_r \frac{dv_r}{dr} - \frac{v_\theta^2}{r} \right] = -\frac{KT}{n} \frac{dn}{dr} + q \left[E + v_\theta B \right] - m v_r \frac{S}{n} \quad (25)$$

(Ref 19:219) where v_θ is the average azimuthal velocity of particles about the ax's of the system. The azimuthal vector component equation is

$$m \left[v_r \frac{dv_\theta}{dr} + \frac{v_r v_\theta}{r} \right] = -q v_r B - m v_\theta \frac{S}{n} \pm \frac{F_c}{n} \quad (26)$$

F_c appears only in this equation because it is azimuthal in direction only. Hence we write it as a scalar in this equation. The sign of F_c depends on whether Eq (26) is written for electrons or ions. Let the electron distribution be chosen as the zero-subscripted distribution in Appendix D. Then F_c should appear as a negative term in the electron equation and as a positive term in the ion equation.

In an axisymmetric system Eq (22) becomes

$$\frac{dB}{dr} = -\mu_0 j_e \quad (27)$$

The azimuthal current density, j_e , can be written so that

$$\frac{dB}{dr} = \mu_0 e [n_e v_e - Z n_i u_e] \quad (28)$$

where e is the electronic charge. The subscripts e and i are introduced to differentiate between the electron and ion distributions. Henceforth v will be used to refer to electron velocities and u to refer to ion velocities.

The electric field equation is

$$\frac{1}{r} \frac{dr E}{dr} = \frac{e}{\epsilon_0} [Z n_i - n_e] \quad (29)$$

where we have rewritten charge density as the sum of the electron and ion charge densities.

We have then a set of simultaneous first order differential equations with r as the independent variable. There are two momentum transfer equations and one continuity equation for each particle distribution, in addition to two Maxwell equations for B and E , for a total of eight equations. The equations are in terms of particle densities, average radial and azimuthal velocities, radial electric field strength, and axial magnetic field strength.

These variables are the unknowns of interest. We wish eventually to study the radial profiles of each. This does not necessarily mean that we must solve each of the

eight equations for one of these unknowns. Several possible changes of variables are considered in the next chapter.

Normalization. Before moving on to the next chapter, wherein attempts are made to solve the eight equations just derived, we introduce normalization of the variables. Normalization eliminates dimensional units and provides very convenient scaling of our particular variables.

For instance, let all velocities be normalized in terms of the mean random velocity of the positive ion:

$$v = v' \sqrt{\frac{3kT_i}{m_i}} \quad (30)$$

where T_i is temperature in degrees Kelvin. The object is to replace all velocities with corresponding primed, dimensionless numbers. For convenience define

$$V = \sqrt{\frac{3kT_i}{m_i}} \quad (31)$$

Let time be normalized in terms of the cyclotron period of the ion near the axis.

$$t = t' \tau \quad (32)$$

$$\tau = \frac{m_i}{ZeB_0} \quad (33)$$

where B_0 is the axial magnetic field strength. It was assumed earlier that B_0 could be specified.

Earlier it was mentioned that one of the goals of this study is to determine theoretically the feasibility of

attaining particle number densities on the order of 10^{20} m^{-3} . Let densities and the density source terms be normalized to

$$n = 10^{20} \text{ m}^{-3} \quad (34)$$

Consistent with the above definitions are the following normalizations:

$$\text{Radius:} \quad r = r' \sqrt{\tau} \quad (35)$$

$$\text{Magnetic field:} \quad B = B' B_o \quad (36)$$

$$\text{Rate of particle creation:} \quad S = \frac{S' n}{\tau} \quad (37)$$

$$\text{Angular frequency:} \quad \omega = \omega' \tau \quad (38)$$

$$\text{Electric field:} \quad E = E' \sqrt{\tau} B_o \quad (39)$$

$$\text{Collision force:} \quad F_c = F_c' \frac{\sqrt{\tau}}{\tau} m_i \quad (40)$$

When these definitions are substituted into the eight equations all dimensions cancel out. Let us then drop all primes, remembering from the above definitions how to recover the real variables. Table I is a compilation of all eight normalized equations, plus F_c , the normalized collision force from Appendix D, after the primes are dropped.

Table I

$$\frac{1}{\pi} \frac{d(\nu n_e v_r)}{d r} = S_e \quad (41)$$

$$\frac{1}{\pi} \frac{d(\nu n_i u_r)}{d r} = S_i \quad (42)$$

$$m_e \left(v_r \frac{d v_r}{d r} - \frac{v_e^2}{r} \right) = - \frac{m_i T_e}{3 T_i} \frac{1}{\pi} \frac{d n_e}{d r} - \frac{m_i}{Z} (E + v_e B) - m_e v_r \frac{S_e}{n_e} \quad (43)$$

$$m_i \left(u_r \frac{d u_r}{d r} - \frac{u_e^2}{r} \right) = - \frac{m_i}{3} \frac{1}{n_i} \frac{d n_i}{d r} + m_i (E + u_e B) - m_i u_r \frac{S_i}{n_i} \quad (44)$$

$$m_e v_r \left(\frac{d v_e}{d r} + \frac{v_e^2}{r} \right) = + \frac{m_i}{Z} v_r B - m_e v_e \frac{S_e}{n_e} - \frac{F_e}{n_e} \quad (45)$$

$$m_i u_r \left(\frac{d u_e}{d r} + \frac{u_e^2}{r} \right) = - m_i u_r B - m_i u_e \frac{S_i}{n_i} + \frac{F_e}{n_i} \quad (46)$$

$$\frac{d B}{d r} = \frac{\mu_0 3 \hbar T_i}{Z e B_0} (n_e v_e - Z n_i u_e) \quad (47)$$

$$\frac{1}{\pi} \frac{d(\nu E)}{d r} = \frac{m_i r}{Z e B_0^2} (Z n_i - n_e) \quad (48)$$

$$F_e = \left(\frac{g_e g_e}{\epsilon_0} \right)^2 \left[\frac{\beta_e \beta_i (m_e + m_i)}{\beta_e m_e + \beta_i m_i} \right] \frac{e n_e \lambda n_i \pi}{2 \pi^{3/2} Z e B_0 [3 K T_i]} \sum_{n=1}^{\infty} \frac{(-1)^{n+1} \rho_0^{2n-1}}{(2n+1)(n-1)!} \quad (49)$$

$$\rho_0 = \pi (\omega_e - \omega_i) \left[\frac{3}{2} \frac{\beta_e m_e}{(\beta_e m_e + \beta_i m_i)} \right]^{1/2} \quad (50)$$

Summary

This chapter is a derivation of a set of time-independent differential equations which describe the macroscopic variables of a system of ions and electrons near equilibrium. It is useful to summarize the assumptions upon which the derivation is based:

1. The system is axisymmetric.
2. Both ions and electrons obey Boltzmann-like distributions and a real plasma can be accurately described by applying their respective distribution functions separately.
3. The magnetic field is axially directed and its strength on axis can be specified.
4. The electric field is radial in direction.
5. Ions and electrons can be inserted into the plasma arbitrarily at any time rate desired. Decelerating drag forces on the two separate distributions arise from collisions between like particles only, and may be treated as average forces.
6. The drag force between electron and ion distributions may be treated as an average volumetric force.
7. Pressure on a single distribution is due only to random collisions between like particles in the distribution.

GSP/PH/69-7

8. The electron and ion temperatures are known
and are uniform across the plasma.

IV. Solving the Differential Equations

Introduction

This chapter describes in detail attempts to develop procedures for the numerical integration of the system of differential equations derived in Chapter III. The objective of these attempts was to select in terms of accuracy and efficiency the best methods for numerical solution of this particular system of equations. Involved are the choice of variables sought as solutions, the adaptation of standard numerical integration techniques to the specific problem, and the writing of computer programs to perform calculations most accurately and efficiently.

First a set of variables is selected and the equations in Table I are solved for the first derivative of one of the variables. Equations for the initial conditions on the variables are derived from the equations written on axis. Sample calculations are made of non-zero initial conditions. These representative values for the initial conditions serve to point out potential sources of error in the computation of the derivatives. Various changes of variables are studied in attempting to eliminate the sources of error. The chapter is concluded with an analysis of the application of numerical integration techniques to the solution of the differential equations.

Choice of Variables

In Chapter III mention is made of which of the variables involved in the system of equations are of interest, but equations are not selected to be solved for specific variables. In this section alternative methods of solving the equations are discussed.

The following macroscopic quantities, as functions of radius, are the objects of this study: n_e , n_i , v_r , v_θ , u_θ , B and E . (The equations in Table I are in terms of the corresponding normalized variables, but the conversions back to the real quantities are simple.) A straightforward approach is to solve each equation for the first derivative with radius of each of these unknowns, but other arrangements of the equations are possible and may be more useful. This chapter is primarily concerned with evolving a set of variables and the solutions for their first derivatives which are most amenable to numerical integration, keeping in mind the limitations imposed by the available numerical techniques and computer technology.

Eq (47) for magnetic field in Table I is apparently already in its most useful form. There are no obvious rearrangements which might improve it.

Consider Eq (45). Move the second term on the left hand side to the right hand side and divide through by $m_e v_r$. The result is a direct expression for dv_θ/dr .

$$\frac{dv_e}{dr} = -\frac{v_e}{r} - \frac{v_e}{v_r n_e} \frac{r S_e}{m_e} + \frac{m_i}{m_e} \left[\frac{B}{Z} - \frac{F_e}{n_e v_r} \right] \quad (51)$$

However, note that

$$\frac{dv_e}{dr} + \frac{v_e}{r} = \frac{1}{r} \frac{d[r v_e]}{dr} \quad (52)$$

Thus, rearranging Eq (45)

$$\frac{d[r v_e]}{dr} = -\frac{r v_e}{v_r n_e} \frac{S_e}{m_e} + \frac{m_i}{m_e} \left[\frac{B}{Z} - \frac{F_e}{n_e v_r} \right] \quad (53)$$

The independent variable, r , is always known exactly in the step-wise numerical integration techniques usually employed with first order differential equations. Therefore, there should be no trouble retrieving v_e from the solution.

Similarly Eq (46) becomes

$$\frac{d r v_e}{dr} = -\frac{r v_e}{u_r n_i} \frac{S_i}{m_i} - \left[\frac{B}{Z} - \frac{F_e}{n_i u_r} \right] \quad (54)$$

Divide Eq (41) by $n_e v_r$ and expand the derivative.

$$\frac{1}{r} + \frac{1}{n_e} \frac{d n_e}{dr} + \frac{1}{v_r} \frac{d v_r}{dr} = \frac{S_e}{n_e v_r} \quad (55)$$

Note that this equation could be solved for the first derivative of either n_e or v_r . For the moment use Eq (55) to eliminate dv_r/dr from Eq (43). Then a solution for dn_e/dr is

$$\frac{dn_e}{dr} = \frac{n_e \left[\frac{v_e^2}{r} + v_r \left[\frac{v_r - 2Se}{r} - \frac{m_i}{Zme} [E + v_e B] \right] \right]}{\left[\frac{1}{3} \frac{T_e}{T_i} \frac{m_i}{m_e} - v_r^2 \right]} \quad (56)$$

Similarly for the ion equation

$$\frac{dn_i}{dr} = \frac{n_i \left[\frac{u_e^2}{r} + u_r \left[\frac{u_r - 2Si}{r} + [E + u_e B] \right] \right]}{\left[\frac{1}{3} - u_r^2 \right]} \quad (57)$$

Assuming that n_e is a wise choice of variable, Eq (55) could be solved for dv_r/dr and the result integrated for v_r directly. However, if $rn_e v_r$ is chosen as a variable, $d(rn_e v_r)/dr$ is rSe , a quantity which has been assumed to be exactly specified. Therefore the differential of $rn_e v_r$ is known exactly, and for this reason it seems a wise choice of variable. Hence,

$$v_r = \frac{rn_e v_r}{rn_e} \quad (58)$$

$$u_r = \frac{rn_i u_r}{rn_i} \quad (59)$$

Eq (48) can be left almost as is,

$$\frac{d[rE]}{dr} = \frac{mir}{Z\epsilon_0 B_0^2} [Zn_i - n_e] \quad (60)$$

The equations in Table I of Chapter III have been rearranged as solutions for the first derivatives of the following variables: $rn_e v_r$, $rn_i u_r$, rv_e , ru_e , B , and rE .

The next logical step is to find the initial conditions on all variables so that the differential equations can be solved.

Initial Conditions

If the numerical integration of the system of differential equations is to be started from zero radius, it is necessary to have a means of computing the numeric values of all variables on axis. Some of the variables are zero by symmetry; those others which are not arbitrarily controlled must be analytically derived. Then standard numerical methods of solving first order simultaneous differential equations can be used to carry on the integration away from the axis.

Some of the initial conditions are immediately evident from symmetry. Recall that the radial and azimuthal velocity terms are averages, or drift velocities, referenced to the axis. Then on axis all the velocities are zero. The electric field must be zero on axis by symmetry also.

Although the azimuthal velocities at $r=0$ must be zero, the angular frequencies of rotation, ω_e and ω_i , can be finite. Indeed in Chapter III it was suggested that such frequencies are constant across the plasma.

Since in Chapter III the magnetic field is normalized to its axial magnitude, B is unity on axis. Recall the assumption that the real value of B on axis, B_0 , can be arbitrarily imposed. It was also assumed that the two

distribution temperatures, T_e and T_i , are known and are uniform across the plasma.

The electron and ion number densities, n_e and n_i , are the remaining initial conditions. Let us seek algebraic solutions for r_e and n_i by solving simultaneously the differential equations as they can be written on axis.

First multiply Eq (55) by r .

$$\frac{r}{r} + \frac{r}{n_e} \frac{dn_e}{dr} + \frac{r}{v_r} \frac{dv_r}{dr} = \frac{r}{v_r} \frac{S_e}{n_e} \quad (61)$$

Take the limit of v_r/r as r goes to zero

$$\lim_{r \rightarrow 0} \frac{v_r}{r} = \frac{dv_r/dr}{dr/dr} = \frac{dv_r}{dr} \quad (62)$$

(Ref 14:262). Since $dn_e/n_e dr$ must be finite on axis, the second term in Eq (61) is zero on axis. Then

$$\frac{2}{r} \frac{v_r}{n_e} = \frac{S_e}{n_e} \quad (63)$$

Reduce Eq (56) to an algebraic equation with no v_r or v_e terms by use of Eqs (61), (62), (63), and

$$w_e = \frac{v_e}{r} \quad (64)$$

The result is

$$\frac{3}{4} \left[\frac{S_e}{n_e} \right]^2 = w_e^2 - \frac{m_i}{Z m_e} \left[w_e + \frac{E}{r} \right] \quad (65)$$

where B has been set equal to one. Similarly for the ion distribution

$$\frac{3}{4} \left[\frac{S_i}{n_i} \right]^2 = \omega_i^2 + \omega_i + \frac{E}{r} \quad (66)$$

At this point it is convenient to make a change of variable for the purposes of the solution for initial conditions. Define as the difference between densities

$$\rho = Zn_i - n_e \quad (67)$$

Also define an average density

$$n = [Zn_i + n_e]/2 \quad (68)$$

As in Eq (62) when r goes to zero,

$$\lim_{r \rightarrow 0} \frac{E}{r} = \frac{dE}{dr} \quad (69)$$

Therefore Eq (60) becomes on axis

$$\frac{2E}{r} = \frac{m_i}{Z\epsilon B_o^2} \rho \quad (70)$$

Define for subsequent use

$$\epsilon = \frac{m_i}{Z\epsilon B_o^2} \quad (71)$$

Turn to Eqs (53) and (54) to see if expressions for ω_e and ω_i can be derived. Using the definition of ω_e , Eq (64), and the initial value of B , Eq (53) becomes

$$2\omega_e = -2\omega_e + \frac{m_i}{m_e} \left[\frac{1}{Z} - \frac{F_c}{n_e V_r} \right] \quad (72)$$

Assume in the normalized expression for F_c in Table I that the first power of the difference $(\omega_e - \omega_i)$ is much greater than any of its higher powers. This assumption will be verified when ω_e and ω_i are solved for. Then approximately

$$F_c = C_f Z_{n_i n_e} [\omega_e - \omega_i] \quad (73)$$

C_f includes all the constants in the first term of the series of the normalized expression for F_c . A glance at Appendix D shows that in a strict sense an unknown, $\ln(n_e)$, is thus included in C_f . However, it happens that the normalization of densities causes $\ln(n_e)$ on axis to be very near zero. When the actual method of computing the axial n_e and n_i is described, it will be shown how the value of $\ln(n_e)$ is corrected in the coefficient C_f .

Using the change of variable previously defined,

$$Z_{n_i n_e} = n^2 - \rho^2/4 \quad (74)$$

Assume for the moment that the relative difference between Z_{n_i} and n_e is so small that

$$\rho^2 \ll n^2 \quad (75)$$

This approximation will be validated. Therefore

$$Z_{n_i} n_e = n^2 \quad (76)$$

Then using Eq (63) solve Eq (53) for ω_e

$$\omega_e = \frac{\frac{2}{Z} + C_f \left[\frac{1}{Z S_i} - \frac{1}{S_e} \right] n^2}{8 \frac{m_e}{m_i} + 4 C_f \left[\frac{1}{S_e} + \frac{m_e}{m_i} \frac{1}{S_i} \right] n^2} \quad (77)$$

Similarly from Eq (54) ω_i on axis is

$$\omega_i = \frac{-2 \frac{m_e}{m_i} + C_f \left[\frac{1}{Z S_i} - \frac{1}{S_e} \right] n^2}{8 \frac{m_e}{m_i} + 4 C_f \left[\frac{1}{S_e} + \frac{m_e}{m_i} \frac{1}{S_i} \right] n^2} \quad (78)$$

The assumption made in Eq (75) also allows the following:

$$\frac{1}{n_e^2} \approx \frac{1}{[n^2 - \rho n]} \quad (79)$$

Expand this result in a binomial series

$$\frac{1}{n^2 \left[1 - \frac{\rho}{n} \right]} = \frac{1 + \frac{\rho}{n} + \frac{3}{4} \frac{\rho^2}{n^2} + \dots}{n^2} \quad (80)$$

Invoking Eq (75) again,

$$\frac{1}{n_e^2} \approx \frac{1}{n^2} \left[1 + \frac{\rho}{n} \right] \quad (81)$$

Similarly for n_i

Table II

<u>Degree of Term</u>	<u>Coefficient</u>
9	$-\mathcal{E} C_F^2 \frac{m_i}{zm_e} \left(\frac{1}{zS_i} - \frac{1}{S_e} \right)^2$
8	0
7	$\frac{8\mathcal{E} C_F}{z} \left(1 + \frac{m_i}{zm_e} \right) \left(\frac{m_e}{m_i} \frac{1}{S_i} + \frac{1}{S_e} \right) + 12\mathcal{E} C_F^2 \left(\frac{m_e}{m_i} \frac{1}{S_i} + \frac{1}{S_e} \right)^2 \left(S_e^2 + \frac{m_i}{zm_e} S_i^2 \right)$
6	$-3C_F \left(\frac{m_e}{m_i} \frac{1}{S_i} + \frac{1}{S_e} \right) \left(S_e^2 - \frac{m_i}{zm_e} S_i^2 \right) - \frac{9}{16} C_F^2 \left(\frac{1}{zS_i} - \frac{1}{S_e} \right)^2 \left(S_e^2 + S_i^2 \right)$
5	$12\mathcal{E} \left(\frac{1}{z^2} + \frac{m_e}{zm_i} \right) + 36\mathcal{E} C_F \frac{m_e}{m_i} \left(\frac{m_e}{m_i} \frac{1}{S_i} + \frac{1}{S_e} \right) \left(S_e^2 + \frac{m_i}{zm_e} S_i^2 \right)$
4	$6C_F \left(\frac{m_i}{m_e} \frac{1}{S_e} + \frac{1}{S_i} \right) \left(\frac{(m_i)^2}{zm_e} S_i^2 + S_e^2 \right) + \frac{3}{z} C_F \left(\frac{1}{zS_i} - \frac{1}{S_e} \right) \left(\frac{S_i^2}{z} - \frac{m_e}{m_i} S_e^2 \right)$
3	$48\mathcal{E} \left(\frac{m_e}{m_i} \right)^2 \left(S_e^2 + \frac{m_i}{zm_e} S_i^2 \right)$
2	$9 \left(\left(\frac{m_e}{m_i} \right)^2 S_e^2 + \frac{S_i^2}{z^2} \right) + 72C_F S_e^2 S_i^2 \left(\frac{m_e}{m_i} \frac{1}{S_i} + \frac{1}{S_e} \right)$
1	0
0	$72 \left(\frac{m_e}{m_i} \right)^2 S_e^2 S_i^2$

$$\frac{1}{n_e^2} \approx \frac{1}{n^2} \left[1 - \frac{\rho}{n} \right] \quad (82)$$

These approximations can be used to replace n_e^{-2} and n_1^{-2} in Eqs (65) and (66). Eq (70) gives E/r in terms of ρ and a constant. Thus Eqs (65) and (66) can both be solved for ρ in terms of n , ω_e , ω_i , S_e , and S_1 . Eq (65) is solved for ρ below as an example.

$$\rho = \frac{-\frac{3}{4} \left[\frac{S_e}{n} \right]^2 + \omega_e^{-2} - \frac{m_i}{Zme} \omega_e}{\frac{3}{4} \frac{S_e^2}{n^3} + \frac{m_i \epsilon}{Zme}} \quad (83)$$

If the solutions for ρ are equated, a ninth degree polynomial in n can be written. Table II is a list of the coefficients of each power of n .

There are methods of solving for the roots of polynomials of any degree (Ref 10:16). However, it is not necessary to solve for all nine roots of the polynomial. We are interested only in those positive roots which correspond to an unnormalized density on the order of 10^{20} m^{-3} . It can be shown that these roots can be found directly.

Approximate Solution. Instead of trying to solve the entire ninth order polynomial for all nine roots of n let us seek an approximate solution for the root, or roots, of interest. Note that the coefficients in Table II are in terms of C_f , ϵ , S_e , and S_1 . C_f and ϵ are the normalized

coefficients of the equations for F_c and $d(rE)/dr$, respectively. S_e and S_i are the normalized source terms on axis. It is very interesting to invent a numerical example which demonstrates how the solution for n depends on these source terms.

Suppose that the unnormalized source terms are on the order of $10^{19} \text{ m}^{-3}/\text{sec}$. That is, if we begin with no density at all and assume no diffusion away from the region of the axis, in ten seconds the number densities of both electrons and ions would be about 10^{20} m^{-3} . Suppose also that S_e and S_i differ by one percent in magnitude. At this point we will not specify which is larger. Let B_0 equal one kilogauss. If now the source terms are normalized, and put into the expression for the coefficients in Table II, the non-zero coefficients assume the following approximate values:

Degree of Coefficient	Value of Coefficient
9	-10^{12}
7	10^{12}
6	10^{-9}
5	10^6
4	10^{-3}
3	10^{-13}
2	10^{-15}
0	10^{-37}

Note that the ninth degree coefficient is the only negative coefficient. An examination of Table II shows that this coefficient must always be negative. The other coefficients are all positive. Since only positive roots of the polynomial interest us, the magnitude of the ninth degree term of the polynomial must always equal the magnitude of the sum of the other nine terms if the polynomial is to sum to zero. For the set of values just computed it is evident that the seventh and ninth degree terms are by far the largest terms in the polynomial. To illustrate, suppose we approximate the polynomial as follows:

$$-10^{12} n^9 + 10^{12} n^7 = 0 \quad (84)$$

The solution is obviously n equal to about one. Hence for this root the other terms of the polynomial are indeed small by comparison and can be neglected. This root translates to an unnormalized average density of about 10^{20} m^{-3} , which is about the size of number densities of interest. Therefore the source terms chosen for this example at least fall in the neighborhood of interesting cases.

* For specified conditions very different from those of the above example, the approximations made should be checked for validity. Nevertheless, if the approximations do hold nearly as well, an approximate expression for n^2 is then available from the ratio of the seventh to the ninth degree coefficients in Table II. It is interesting to examine this ratio, using only the first term of the

seventh degree coefficient since it is much larger than the other term.

$$n^2 = \frac{8 \left[1 + \frac{m_i}{Zm_e} \right] \frac{m_e}{m_i}}{C_f S_e \left[\frac{1}{ZS_i} - \frac{1}{S_e} \right]^2} \quad (85)$$

Neglect terms of order m_e/m_i compared to one.

$$n^2 \approx \frac{8 S_e}{Z C_f \left[\frac{S_e - Z S_i}{Z S_i} \right]^2} \quad (86)$$

Note that n is inversely proportional to the relative difference between S_e and ZS_i and proportional to the square root of the source terms.

It is to be stressed that the above approximate expression for n^2 may not be valid for all imposed initial conditions. It will be used only as a means to estimate the root of interest. The complete polynomial, without approximations, should be computed to insure that it is near zero. If it is, the solution for n can be refined by iterative correction schemes. The Newton-Raphson method of finding a root of a polynomial is quite useful and quick when a good estimate of the root is available (Ref 10:630). It is well suited to iterative computer techniques.

The C_f used in Eq (86) to compute the first trial value for n was computed with $\ln(n_e)$ equal to zero. Then in every iteration of the Newton-Raphson method $\ln(n)$ should

be used where $\ln(n_e)$ appears in C_f . $\ln(n_e)$ is not one of the larger terms in $\ln(\Lambda)$. (See Appendix D.) Then the very small difference between $\ln(n_e)$ and $\ln(n)$ cannot have a great effect on the accurate calculation of C_f . Hence rapid convergence of the iterative solution for the root of interest is realized.

Origins of Error

It is prudent at this point to look at the physics of the situation and search for any arithmetic operations in the eight equations which might introduce error. Since the intent is to use numerical integration techniques to solve the equations in Table I, it is imperative that the differentials chosen in this chapter be computed as accurately as possible. Therefore it is interesting to study the effects of the error associated with each term of the differentials and to investigate how such errors might be induced.

In the electric field equation the derivative depends on the difference between electron and ion charge densities; both are integrated variables and thus subject to error. Any computer language has only a finite number of significant digits it can assign to any single variable. In Fortran IV, for example, the maximum number of digits available to any real variable is sixteen. (Ref 9:6) If Zn_1 and n_e are nearly equal on the average, their difference may not appear except in the last few significant figures of either. The accuracy of rE can thus be severely limited. It is expected, in fact, that the net charge

densities in a plasma in equilibrium is nearly zero. The only way of determining if it is feasible to calculate rE by Eq (60) is to make some representative calculations of the difference between Zn_1 and n_e .

Recall the assumption that the axial magnetic field is to be imposed. The electric field can arise only from the relative motion between the two oppositely charged distributions. The average azimuthal rotation of a charged distribution results in a radial force on the distribution in the presence of an axial magnetic field. Because the electrons and ions are oppositely charged, the radial forces thus generated tend to drive the two distributions in opposite radial directions. A radial electric field appears to prohibit this separation. Thus a cancellation of force terms is involved in the terms $(E + v_\theta B)$ and $(E + u_\theta B)$. The potential for a prohibiting loss of accuracy in either or both of these Lorentz force terms exists if E is nearly equal in magnitude to either $v_\theta B$ or $u_\theta B$.

Three terms in the eight differential equations have been identified as potential sources of error. It is expected that the calculation of these terms might require computing a relatively small difference between two nearly equal numbers. The loss of significance amounts to a loss of accuracy in these differences in computer calculations.

The severity of accuracy loss in the sensitive terms cannot really be judged until accurate numeric values for the variables involved in each term are available. Nor can

the effects of the error in these terms on the accuracy of the differentials be determined until the relative magnitudes of all the terms in each equation can be estimated.

Numerical Example. To ascertain whether the above problems can arise it is again useful to go through a numerical example. Suppose that a cylindrical plasma sustains a voltage as high as 10,000 volts across a radius on the order of 10 cm. Suppose also that the electric field strength is approximately linear with radius. Then at 5 cm from the axis the electric field strength is about 1000 volts/cm. This is quite a high electric field for an ionized gas to sustain.

From Eq (29) the difference between the unnormalized electron and ion densities corresponding to this electric field is about $2.2 \times 10^{15} \text{ m}^{-3}$. If we assume that the mean particle density is as high as 10^{20} m^{-3} , the relative difference between Zn_1 and n_e is about 10^{-5} . For smaller electric fields this difference is even smaller.

Note that by the equations chosen as solutions for the derivatives of n_e and n_i the densities are solved for separately. It then becomes necessary to compute their difference in the electric field equation. So in computer calculations, where the densities can only be known to a finite number of significant places, their difference is known accurately to fewer significant places than either density because the first few significant places are cancelled out. In the example above five significant figures

are lost every time the difference is calculated. For smaller electric fields or higher average densities the relative differences between electron and ion densities is even smaller.

It is possible from the initial condition equations derived earlier to find an analytic expression for the term $(E + v_\theta B)$ on axis. Immediately, since B on axis is one, the term is simply $(E + r\omega_e)$. Let us find an expression for this term on axis and find its size relative to v_θ . The conclusions can be qualitatively extended for the rest of the plasma and to the equivalent term in the ion equation.

By Eqs (70) and (71), in terms of normalized variables,

$$E = \frac{Z}{2} r \rho \quad (87)$$

Then the term of interest relative to v_θ is

$$\begin{aligned} \frac{E + r\omega_e}{r\omega_e} &= \left[Z \frac{m_e}{m_i} r\omega_e^2 - r\omega_e + r\omega_e \right] / r\omega_e \\ &= Z \frac{m_e}{m_i} \omega_e \end{aligned} \quad (88)$$

Recall that ω_e has been normalized to the ion cyclotron frequency, and that it is used here as an average frequency of rotation for the entire electron distribution. Hence the ω_e above is less than one. Thus, since m_e is much less than m_i , E and $r\omega_e$ are nearly equal in magnitude, and there is a cancellation of the first significant figures in

taking their difference. Similar results hold for the term $(E + u_\theta B)$.

The significance of the above examples and arguments is that there can easily be a severe loss of accuracy in computing the first derivatives of n_e and n_i . Recall that significant figures were lost in the electric field equation. Now we find that additional significant figures can be lost in the Lorentz force terms. Thus n_e and n_i cannot be accurately computed to even the limited number of places available in the computer.

It seems then that some means should be sought to solve for the difference between Zn_i and n_e directly rather than subtracting them every time the derivative of rE is computed. That is, ρ should be chosen as one of the variables of the system such that it can be solved for directly. The next section discusses such a change of variable.

Change of Variable

It is suggested in the last section that instead of integrating for n_e and n_i it would be wise to solve directly for the difference between them. It was shown that a severe loss of accuracy could ensue from subtracting the two densities. To solve for the first derivative of ρ ,

$$\frac{d\rho}{dr} = Z \frac{dn_i}{dr} - \frac{dne}{dr} \quad (89)$$

By definition of n we could choose it as the other density variable.

$$\frac{dn}{dr} = \frac{1}{2} \left[Z \frac{dn_1}{dr} + \frac{dne}{dr} \right] \quad (90)$$

Thus, in principle, we need only add or subtract Eqs (56) and (57) to make the change of variables. However, note that there is no cancellation of any equal terms accomplished by the subtraction of dne/dr from Zdn_1/dr . Thus nothing has been done to eliminate the large common factors shared by Zn_1 and n_e .

It has been shown then why an obvious change of variables does not remedy the basic problem with this set of equations. The problem is the loss of accuracy incurred by subtracting with the computer nearly equal terms. The next section explains how this type of error makes impossible the numerical integration of differential equations.

Numerical Integration

Many approximate methods of numerically integrating the general first order differential equation have been invented. The oldest and simplest are Euler's method and its modification (Ref 15:310). They both essentially make linear extrapolations from one known value of a function to a new value by multiplying the derivative of the function by an increment of the independent variable. More elegant methods such as Approximating Polynomials (Ref 15:358), and Milne (Ref 15:353) employ the extrapolation method more cleverly, but the use of them can also be limited by this approximation.

The Milne method is an example of the general predictor-corrector scheme. The two basic equations it uses are

$$\text{Predictor: } y_{n+1} = y_{n-3} + \frac{4h}{3} 2y'_{n-2} - y'_{n-1} + 2y'_n \quad (91)$$

$$\text{Corrector: } y_{n+1} = y_{n-1} + \frac{h}{3} y'_{n-1} + 4y'_n + y'_{n+1} \quad (92)$$

where y_{n+1} is the value of the dependent variable being sought. The subscripts denote the number of steps by which the independent variable has been incremented. The primed quantities are the first derivatives of the dependent variable. The predictor equation provides an estimate of y_{n+1} at the next incremented value of the independent variable based on the behavior of the function at previous increments. The corrector equation calculates y_{n+1} over and over until successive answers agree to within some accepted error.

Note that in the predictor equation the values of y at four previous increments are required. Some starting solution is usually required to calculate the first three values of every dependent variable, and, of course, the initial conditions for all variables must be known. Runge-Kutta is a very popular method of obtaining the three starting values from a knowledge of the initial conditions. Runge-Kutta is essentially derived from a truncation of the Newton series for forward interpolation (Ref 15:56), and therefore imposes the approximation of linearity.

The Runge-Kutta method was applied to the eight differential equations for several sets of imposed conditions to obtain the first three solutions for all the variables selected earlier, and the Milne method was applied at the fourth step as explained above. Initial conditions were computed as described earlier in the chapter. As the corrector equation was applied repeatedly at the fourth step, the values of the variables did not converge, but rather increased or decreased beyond reasonable limits. Within a few iterations the two densities decreased by several orders of magnitude, and E and the four velocities increased in a like manner.

Apparently the sensitive differences in the density equations, and the electric field equation were computed erroneously due to small errors in the terms involved in the differences. The derivatives of these terms were then inaccurately calculated since the differences occurred in the last significant figures of the variables. The repeated application of the corrector equation served to amplify the errors rather than improve the predicted values of the variables.

Series Expansions. Suppose the exact initial values of all non-zero variables were available. It might then be possible to expand all variables about the axis in algebraic series in terms of r . If the variables could be expanded to enough terms so that very accurate values of each a short distance off axis were available, the three

starting solutions could be had by computing each series at three different radii.

The Taylor Series method (Ref 15:328) is often used to begin from initial conditions the numerical solution of any order differential equation. It is based on the expansion of the dependent variables into infinite series in powers of the independent variable.

$$y_i(x) = y_i(x_0) + y_i'(x_0)[x-x_0] + \frac{y_i''}{2}(x_0)[x-x_0]^2 + \dots \quad (93)$$

where $y_i(x_0)$ is the initial condition on y_i at x_0 . The primary limitation on this method is usually the excessive labor involved in solving algebraically for the higher order derivations. However, if $(x-x_0)$ is kept small, a variable might be represented accurately by only two or three terms of a Taylor series.

The usual procedure of computing the coefficients of the $(x-x_0)$ terms is to substitute the truncated series for each variable into the set of differential equations and solve simultaneously for the coefficients. Each differential equation reduces to an algebraic equation which can be subdivided into equations of the coefficients of like powers $(x-x_0)$. There are always as many coefficient equations as coefficients if there is a differential equation for each variable. In principle the set of simultaneous coefficient equations can always be solved, often numerically, for the numerical values of the coefficients.

Assume then that it is possible to expand each of the variables, using n and ρ as density variables, into series which represent the variables a short distance from the axis to greater accuracy than the digital computer is capable of carrying. Each variable could be computed analytically to some distance R_1 . Then another expansion could be made about R_1 , and a whole new set of coefficients for each variable simultaneously computed. The new expansion could be checked by calculating the variable back toward the axis and comparing the radial profiles of the variables expressed by both series. This process could be extended in short segments to any radius. A possible limitation would be a region where all the variables become rapidly changing functions of r , in which case the number of terms in the Taylor series necessary to represent each variable accurately might be prohibitive.

Let us then investigate the possibility of applying such a contrived method to the eight differential equations. Immediately, the equations are non-linear; that is, products of variables appear in them. So the simultaneous coefficient equations would be non-linear. Although the methods of solving simultaneous linear equations are well established, the generalized methods pertaining to non-linear equations become exceedingly complex for more than just two or three equations.

However, the identical problem arises which prevented the change of variables to n and ρ in the last section.

Note that the coefficients of the n and ρ series would still have to come from the simultaneous solution of Eqs (56) and (57). It was found before when solving for $d\rho/dr$ that no cancellation of terms in Eqs (56) and (57) could be accomplished. Hence the large common factor between n_e and n_1 could not be eliminated. This same problem would appear in the simultaneous solution for the series coefficients of ρ . Terms like $(E + v_\theta B)$ and $(E + u_\theta B)$ would only be translated into terms involving the coefficients of E , v_θ , u_θ , and B . The difficulty of computing relatively small differences between large numbers would remain. This dilemma was actually verified by expansion of all variables as described above.

In this section it has been shown how even small errors in the variables make the numerical integration of the equations by such methods as Runge-Kutta and Milne impossible. The Taylor method has been proposed and it has been demonstrated not feasible also.

Summary

This chapter deals essentially with the failure to find a method of accurately integrating the equations derived in Chapter III. A set of variables is first chosen from which the variables of interest can be algebraically computed. The sources of error are identified in the terms of the differentials of these variables so that the reader can understand the purpose of the subsequent arguments.

The differential equations are written for $r=0$, and expressions for initial conditions on all variables are derived from them. Such solutions are required before numerical integration methods can be applied. The initial condition equations are used, with some typical values of the specified constants, to illustrate the severity of a major obstacle to the solution of the equations away from the axis. It is found that a property of the system of equation is the very small relative difference on axis between n_e and Zn_i .

The results of the application of several common integration methods are reported. The behavior of the variables under the Milne iterative integration scheme confirms that some of the differentials are subject to a severe loss of accuracy. The electric field equation is most immediately affected by the loss of accuracy in the difference between the particle densities. The error in E causes the differentials of the density terms to be erroneously computed. The most important reason for this is the equality of $v B$ with $(-E)$, and $u B$ with $(-E)$. The effect of error in the terms is amplified by the cancellation of their most significant parts.

No rearrangement of the differential equations could be found such that the cancellation of the common factors between nearly equal terms can be performed analytically. The equations came originally from the separate application of the Boltzmann equation to the electron and ion

GSP/PH/69-7

distributions. It is this separate consideration of the two types of particles which causes the dilemma at hand. The two distributions cannot be handled separately. The electric field equation and the force term F_c unavoidably tie the two together.

V. Conclusion

This chapter proposes recommendations for continued study in the areas discussed in Chapters II through IV. Plans have been already made at the Plasma Physics Research Laboratory of the Aerospace Research Laboratories to formulate methods for overcoming the difficulties explained in Chapter IV, and these plans are reported.

Displaced-Coil Configuration

The study of the magnetic field of the displaced-coil configuration as reported in Chapter II could be greatly expanded. It is limited in validity by the approximations of infinitely-thin coils in an infinitely extended, straight arrangement. It would be useful to devise computer programs similar to those described in Appendices B and C to map the magnetic field of a system of real solenoids arranged as in Fig. 1. The general solenoidal magnetic coil can be treated mathematically just as the single loop of current. Accurate and convenient computer programs have been written to compute the magnetic field of round coils anywhere outside the current windings (Refs 3 and 4).

Besides the additional parameters introduced in using real coils, new variables would arise due to the toroidal arrangement. The curvature of the axis about which the coils are placed would obviously destroy the azimuthal symmetry of the magnetic field. The gradients in field

strength transverse to the general direction of the magnetic field should increase. The most profound effect would probably be on the cyclic rotation of the B lines.

In Chapter II it was demonstrated that such characteristics as longitudinal and transverse gradients of magnetic strength, the ratio of transverse to axial B vector components, and the rotation of B lines are functions of the spatial parameters of the coil configuration of Fig. 2. Very broad conclusions were drawn about the feasibility of selecting specific field characteristics by adjusting these spatial parameters. However, should a toroidal device such as that depicted in Fig. 1 be found promising for plasma containment, some procedure will be needed to design magnetic fields with specified characteristics.

The choice of exact sizes and shapes of solenoids are somewhat limited by what is commercially available. The designer would then have to rely primarily on the spatial arrangement of the coils. Computer techniques probably would be the best tools for finding directly what configuration of available solenoids would yield a magnetic field most nearly like that desired. Many of the computation techniques developed in Appendices A, B, and C would be adaptable in such procedures. Another thesis done in cooperation with the Plasma Physics Research Laboratory reports the attempts of Capt. D. B. Taylor to design coil configurations generating specific magnetic fields by

using standard coils (Ref 17:1).

Indirect Solution of Differential Equations

It became evident in Chapter IV that essentially only one difficulty prevents the direct numerical integration of the differential equations derived in Chapter III. It is a characteristic of the nearly equilibrium plasma that the relative difference between ion and electron number densities is extremely small. No change of variables could be found to eliminate the necessity of subtracting the nearly equal densities. The loss of accuracy in the differences is reflected in the erroneous calculation of important differentials.

Lt. Col. Wingerson has proposed an alternative to solving the equations simultaneously from initial conditions only. It involves a mating of theoretical prediction and experimental verification. Instead of trying to compute the difference between ion and electron densities, it is proposed that the difference be imposed on the equations as a radial function. This would be equivalent to specifying the radial electric field. On the basis of this function and the arbitrary injection of charged particles the system of differential equations might be solved for the variables of interest.

These variables can also be indirectly measured in real plasmas. Plasma probe technology is such that particle densities and rotational velocities are measurable to at least an order of magnitude (Ref 6:1). From a

knowledge of the radial density profiles the continuity equations can be used to compute the radial drift velocities. Although the magnetic strength in a hot plasma cannot be measured directly, the difference between the field due to a set of magnetic coils in a vacuum and in the presence of a plasma can be predicted (Ref 12:73). So the strength of the magnetic field associated with a plasma can be calculated indirectly. Temperatures for both electrons and ions are also available by probe measurement.

Thus all the variables which appear in the differential equations can be measured in a real plasma. Careful comparison of the mathematical solutions and the measurements could show whether the electric field imposed mathematically is consistent with reality. The most important indication would be whether the shape of the radial electric field profile is reasonable, rather than whether the absolute value of the field at any point is exact. The contour of the electric field would indicate what type of series expansion would represent the field most accurately. Then as suggested in Chapter IV all other variables could be expanded in series consistent with the electric field function, and the entire set of equations solved simultaneously for the coefficients of each variable's expansion.

The Plasma Physics Research Laboratory has constructed an axisymmetric plasma containment device called the ELMAX. ELMAX is equipped with Langmuir probes and the associated electronics to measure radial profiles of plasma

GSP/PH/69-7

temperatures, number densities, and rotational frequencies. Lt. Col. Wingerson plans to use the ELMAX to obtain the measured variables. The configuration of the device is similar to the system hypothesized in this paper; it has an axial magnetic field, and gases can be added to the running plasma along the axis of the system. Thus the equations of Chapter III should describe macroscopic phenomena in ELMAX reasonably well.

Bibliography

1. Abramowitz, Milton and I. A. Stegun, editors. Handbook of Mathematical Functions. Washington: National Bureau of Standards, 1964.
2. Bishop, Amasa S. Project Sherwood. Reading, Mass.: Addison-Wesley Press, Inc., 1958.
3. Brown, Gerald V., et al. Axial and Radial Magnetic Fields of Thick, Finite-Length Solenoids. NASA Technical Report R-170. Washington: National Aeronautics and Space Administration, December 1963.
4. Brown, Gerald V. and Lawrence Flax. Superposition Calculation of Thick Solenoid Fields From Semi-Infinite Solenoid Tables. NASA Technical Note D-2494. Washington: National Aeronautics and Space Administration, September 1964.
5. D'Angelo, N. and N. Rynn. Physics of Fluids, 4: 275 (1961).
6. Edmonds, Walter R. Plasma Diagnostics on the ELMAX. Unpublished Thesis. Wright-Patterson Air Force Base. Ohio: Air Force Institute of Technology, June 1969.
7. Gartenhaus, S. Elements of Plasma Physics. New York: Holt, Rinehart, and Winston, 1964.
8. Hodgman, C. D., editor. Mathematical Tables from Handbook of Chemistry and Physics. Cleveland: Chemical Rubber Publishing Co., 1959.
9. IBM. FORTRAN IV Language. IBM Technical Manual. New York: IBM Corporation, December 1965.
10. Korn, Granino A. and T. M. Korn. Mathematical Handbook for Scientists and Engineers. New York: MacMillan Co., 1961.
11. Lencioni, P. E., et al. Physics of Fluids, 2: 1115-25 (May 1968).
12. Lovberg, R. H. "Magnetic Probes." Plasma Diagnostic Techniques, ed. R. H. Huddlestone and S. L. Leonard. New York: Academic Press, 1965.
13. Morse, R. L., et al. Plasma Physics, 10: 543-9 (May 1968).

14. Rainville, Earl D. Unified Calculus and Analytic Geometry. New York: MacMillan Co., 1961.
15. Scarborough, James B. Numerical Mathematical Analysis. Baltimore: The Johns Hopkins Press, 1930.
16. Spitzer, Lyman, Jr. Physics of Fully Ionized Gases (Second Edition). New York: John Wiley and Sons, 1967.
17. Taylor, David B. Synthesis of Arbitrary Axial Magnetic Fields with Standard Coils. Unpublished Thesis. Wright-Patterson Air Force Base, Ohio: Air Force Institute of Technology, June 1965.
18. Thompson, W. B. An Introduction to Plasma Physics. Oxford: Permagon Press, 1962.
19. Uman, Martin A. Introduction to Plasma Physics. New York: McGraw-Hill Book Co., 1964.
20. Van Bladel, J. Electromagnetic Fields. New York: McGraw-Hill Book Co., 1964.

Appendix A

Equations of the Displaced-Coil ConfigurationThin Loop Equations

The radial and axial components of the B field of an infinitely-thin loop of current in cylindrical coordinates are

$$B_r = \frac{\mu_0 I}{2\pi} \frac{z}{r \left[(a+r)^2 + z^2 \right]^{1/2}} \left[-K + \frac{[a^2 + r^2 + z^2]}{[a-r]^2 + z^2} E \right] \quad (94)$$

$$B_z = \frac{\mu_0 I}{2\pi} \frac{1}{\left[(a+r)^2 + z^2 \right]^{1/2}} \left[K + \frac{a^2 - r^2 - z^2}{[a-r]^2 + z^2} E \right] \quad (95)$$

(Ref 20:155), where the axis of the loop is the Z axis of the coordinate system. The azimuthal component of the field is zero by symmetry. "I" is the current; "a" is the radius of the loop in meters; and K and E are the complete elliptic integrals of the first and second kind, respectively.

Normalization. Let us normalize units such that $\mu_0 I / 2\pi a$ is equal to unity. Then B is a dimensionless number. All coordinates are measured as fractions of the radius of the loop.

Elliptic Integrals. The elliptic integrals K and E are defined by the relations

$$K = \int_0^{\pi/2} \frac{d\theta}{\left[1 - k^2 \sin^2 \theta \right]^{1/2}} \quad (96)$$

$$E = \int [1 - k^2 \sin^2 \theta]^{1/2} d\theta \quad (97)$$

where k , called the modulus of the integral, is given by

$$k = \left[\frac{4ar}{[a+r]^2 + z^2} \right]^{1/2} \quad (98)$$

The complementary modulus ck is defined such that

$$CK^2 + K^2 = 1 \quad (99)$$

The elliptic integrals can be expanded into polynomial approximations of various numbers of terms. Two expansions which are within 2×10^{-8} of the true values of K and E for any given k are given below (Ref 1:591).

$$K[ck] = [a_0 + a_1 CK^2 + a_2 CK^4 + a_3 CK^6 + a_4 CK^8] + [b_0 + b_1 CK^2 + b_2 CK^4 + b_3 CK^6 + b_4 CK^8] \ln[1/ck] \quad (100)$$

$$E[ck] = [1 + c_1 CK^2 + c_2 CK^4 + c_3 CK^6 + c_4 CK^8] + [d_1 CK^2 + d_2 CK^4 + d_3 CK^6 + d_4 CK^8] \ln[1/ck] \quad (101)$$

These approximations are useful because of the ability of the digital computer to handle such calculations with great speed.

Singularities. As mentioned above, k must be less than one. The cylindrical coordinates corresponding to k equal to one are r equal to one and z equal to zero, as can be seen immediately from Eq (98). These are the

coordinates of the conducting loop itself. This is expected since any conductor is a singularity in the magnetic field. Otherwise the equations for B_r and B_z are valid for any coordinates r and z , r not equal to zero.

Superposition of Coil Fields

The principle of superposition is exercised to find the magnetic field at any point due to the fields of a number of separate coils. Fields of several coils can be considered together at a point by adding vectorially the \underline{B} vector from each. This is most conveniently accomplished by adding parallel components. An orthogonal coordinate system is defined in Chapter II relative to the coil configuration.

Position Relative to a Coil. The axial distance from any point to the plane of each coil is easily found. It is simply the Z coordinate of the point relative to the system axes plus or minus an integral multiple of the distance between the planes of the coils. The X and Y coordinates relative to an individual coil depend on the position of the center of that coil with respect to the system axes. If the transverse coordinates of a point are X and Y , the coordinates relative to a coil whose center lies at "disp" off the axis, and at an angle "alpha" from the X axis are

$$X_c = X - \text{disp} \cos \alpha$$

$$Y_c = Y - \text{disp} \sin \alpha$$

(102)

Hence, the radial distance from the center of the coil to the point is

$$R_c = \left[X_c^2 + Y_c^2 \right]^{1/2} \quad (103)$$

Thus the R and Z distances can be found for calculation of the magnitudes B_r and B_z of the field of any coil at a given point.

Summation of Components. The B_z components from each coil are added since they are parallel. The B_r components must be divided into B_x and B_y components which are parallel in direction to the system axes.

The directions of the B_r from the coils are radial outward from the centers of the coils to the point under consideration. The B_r are divided via multiplication by direction cosines:

$$B_x = B_r \frac{X_c}{R_c} \quad (104)$$

$$B_y = B_r \frac{Y_c}{R_c} \quad (105)$$

In summary, approximate expressions for the axial and transverse components of B for a single thin loop have been derived. A coordinate system is used as the basis for dividing these components into B_x , B_y , and B_z components. Thus the fields of separate coils are added vectorially at a point.

Appendix B

The Subroutine Field

This appendix describes a subroutine called "Field" which is designed to provide the magnitude and the direction of the magnetic strength vector \underline{B} at any point in the field of the displaced-coil configuration. The origins of the requirement for the subroutine are detailed in Chapter II. The objectives and criteria for design are stated here. The method of computation is explained, and operating instructions are provided. Finally, the effectiveness of the subroutine is evaluated.

Fig. 8 is a flow diagram of Field, and Fig. 9 is a listing of the computer code. Table III defines the Fortran variable names used in Field.

Objectives and Criteria

B_m and Direction Cosines. In Chapter II it is determined that RTA, the ratio of transverse to axial vector components, and the uniformity of B_m , the magnitude of \underline{B} , should be studied. Also, the integration of field lines requires the direction cosines of \underline{B} . It is the objective of Field to supply B_m and the three direction cosines of \underline{B} at any point in the generalized displaced-coil configuration.

RTA is the square root of the sum of the squares of the transverse direction cosines. The uniformity of B_m can

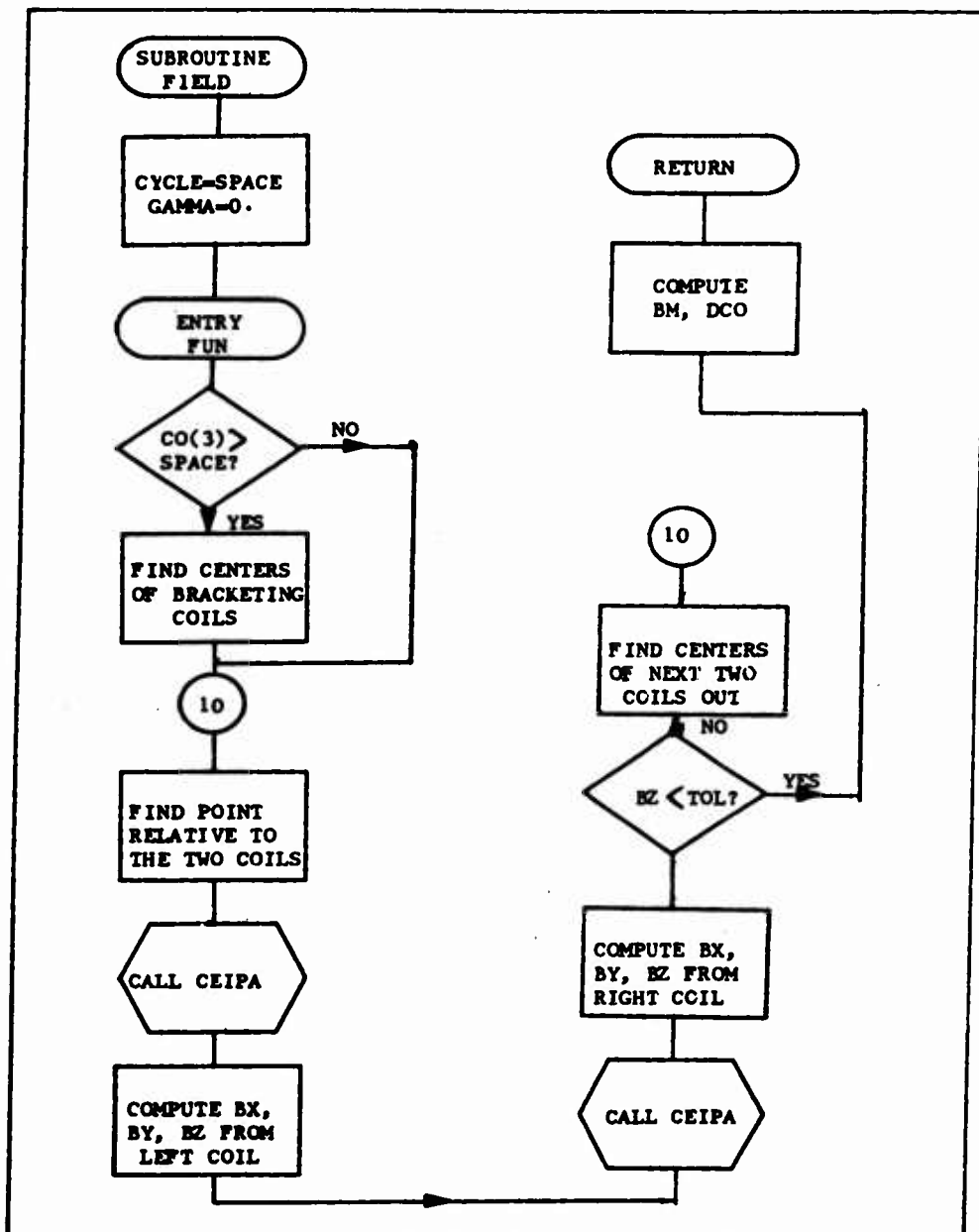


Fig. 8. Flow Diagram of Field

```

SIBFTC FIELD. DECK
  SUBROUTINE FIELD(CO,DCO,BM,SPACE,DISP,ALPHA)
  DIMENSION CO(3),DCO(3)
  ALPHAR=ALPHA/57.3
  TOL=.001
  GAMMA=0.
  CYCLE=SPACE
  ENTRY FUN(N,S,CO,DCO)
C TEST AXIAL COORDINATE OF POINT
  IF (CO(3)-CYCLE) 2,3,3
C IF ANOTHER LOOP HAS BEEN PASSED.....
  3 CYCLE =CYCLE+SPACE
  GAMMA=GAMMA+ALPHAR
  2 CHI=GAMMA
  PSI=GAMMA+ALPHAR
C FIND Z COORDINATES RELATIVE TO NEAREST LOOPS
  ZLEF=CO(3)-CYCLE
  ZRIT=ZLEF-SPACE
  BX=0.
  BY=0.
  BZ=0.
C FIND X-Y COORDINATES RELATIVE TO TWO LOOPS
  10 X =CO(1)-DISP*COS(CHI)
  Y =CO(2)-DISP*SIN(CHI)
  R2=X*X+Y*Y
  R=SQRT(R2)
  Z2=ZLEF*ZLEF
  TOP1=1.+R2+Z2
  TOP2=(1.-R2-Z2)
  BOT1=SQRT((1.+R)*(1.+R)+Z2)
  BOT2=(1.-R)*(1.-R)+Z2
  AK=4.*R/((1.+R)*(1.+R)+Z2)
  CALL CEIPA(AK,FEI,SEI)
  BR1=(ZLEF/RL/BOT1)*(-FEI+TOP1/BOT2*SEI)
  BZ1=(FEI+TOP2/BOT2*SEI)/BOT1
  X =CO(1)-DISP*COS(PSI)
  Y =CO(2)-DISP*SIN(PSI)
  R2=X*X+Y*Y
  R=SQRT(R2)
  Z2=ZRIT*ZRIT
  TOP1=1.+R2+Z2
  TOP2=(1.-R2-Z2)
  BOT1=SQRT((1.+R)*(1.+R)+Z2)
  BOT2=(1.-R)*(1.-R)+Z2
  AK=4.*R/((1.+R)*(1.+R)+Z2)
  CALL CEIPA(AK,FEI,SEI)
  BR2=(ZRIT/RR/BOT1)*(-FEI+TOP1/BOT2*SEI)
  BZ2=(FEI+TOP2/BOT2*SEI)/BOT1

```

Fig. 9. Listing of Field

```
BX=BX+X1/RL*BR1+X2/RR*BR2
BY=BY+Y1/RL*BR1+Y2/RR*BR2
BZ=BZ+BZ1+BZ2
C TEST SIZES OF AXIAL CONTRIBUTIONS
IF(BZ1-TOL*BZ) 21,21,29
IF(BZ2-TOL*BZ) 22,22,29
C IF MORE COILS NEED TO BE CONSIDERED....
29 ZLEF=ZLEF+SPACE
ZRIT=ZRIT-SPACE
CHI=CHI-ALPHAR
PSI=PSI+ALPHAR
GO TO 10
22 CONTINUE
BM=SQRT(BX*BX+BY*BY+BZ*BZ)
DCO(1)=BX/BM
DCO(2)=BY/BM
DCO(3)=BZ/BM
RETURN
END
```

Fig. 9. Listing of Field, (cont.)

Table III

Definitions of Fortran Variables in Field

Fortran Name	Definitions
AK	Modulus of elliptic integrals
ALPHAR	Alpha in radians
BX, BY, BZ	Vector components of <u>B</u>
BR1, BR2	Transverse terms of <u>B</u> from a coil pair
BZ1, BZ2	Axial terms of <u>B</u> from a coil pair
CHI, PSI	Azimuthal coordinates relative to a coil pair
CK	Complementary modulus of elliptic integrals
CO	3-matrix of position coordinates
CYCLE	Integral multiple of space
DCO	3-matrix of direction cosines
FEI, SEI	Elliptic integrals, first and second kind
GAMMA	Integral multiple of ALPHAR
N	Number of dimensions (3)
R2, Z2	Squared radial and axial distances
RL, RR	Radial distances from point to coil centers
S	Integral length of <u>B</u> line
TOL	Parameter of accuracy required of Bz term
TOP1, TOP2, BOT1, BOT2	Terms in the equations for Br, Bz

Table III (cont.)

Definitions of Fortran Variables in Field

Fortran Name	Definitions
X, Y, ZLEF, ZRIT	Field point coordinates relative to a coil pair

be studied by computing B_m as a function of changing radial and axial position. For convenience and generality, therefore, Field is written as a subroutine to be called by any program which requires the magnitude and direction of \underline{B} .

Field is designed to provide for the control of errors of approximation. The necessity for error control arises primarily from the possibility that in an integration process using the output of Field errors may be cumulative. For this reason the maximum errors in the direction cosines are firmly under control.

Method of Calculation

This section explains the application of previously derived equations to the objectives outlined above. It also describes the mechanism of error control.

Vector Component Computation. Equations are developed in Appendix A for the normalized components of \underline{B} in the field of a single loop of current. The coordinates of both the field point and the coil center must be known in order to apply these equations.

Adding Components. Field initially determines from the coordinates of the specified point the coordinates of the centers of the two coils which bracket the point. Calculations of vector components are carried out on one pair of coils at a time, beginning with the pair closest to the point. Pairs successively farther out from the point in both axial directions are considered in turn. The pairs

of vector components are added to the subtotals of Bx, By, and Bz as they are calculated.

Testing Axial Components. The individual axial components are expected to decrease with increasing distance between the point and the coil. Field tests each axial contribution against a value called "tol." Tol is an error parameter defined as the minimum relative size of axial contribution to be considered. It is approximately equal to the difference between the total axial strength at a point in an infinite system of coils and the total of contributions from a finite number of coils.

If both axial terms from a pair of coils are not smaller than tol, Field considers the outer next pair of coils. If the test is met, however, the additive process is terminated. The absolute vector magnitude and the direction cosines are computed. Control is returned to the calling program.

Operating Instructions

The following control statement must be placed in any program calling Field:

DIMENSION CO(3),DCO(3)

where CO is the array of point coordinates, and DCO is the array of direction cosines. Space, disp, and alpha must be defined, and N should be set equal to the integer three in the calling program.

The first time Field is called for a new combination of geometric parameters the following statement is appropriate:

```
CALL FIELD(CO,DC0,BM,SPACE,DISP,ALPHA)
```

Bm and the direction cosines are available in the argument list upon return from Field. This statement must be used if Bm is required at each point.

If Field is serving a line integration routine, the following statement should be used for each integration step after the above statement has been used once:

```
CALL FUN(N,S,CO,DC0)
```

Error Control. Tol is set within Field to a value which insures a maximum error in Bm of one tenth of one percent. If a lesser error is desired, tol can be reset within Field.

Evaluation of Effectiveness

This section is an evaluation of how well Field can be expected to meet the objectives and criteria previously set down. Any stated observations are based on experience in using Field.

Limitations on accuracy of results from Field will be considered first. The absolute limitation upon accuracy arises from the approximate method of computing the complete elliptic integrals. It is noted in Appendix A that the method chosen has a maximum error of 2×10^{-8} in each integral calculation. It is therefore concluded from

a study of the component equations of Appendix A that the minimum meaningful tol that should be considered is 10^{-7} .

The specification of tol should be a compromise between desires for accuracy and economy of computer time. It is advised that a reduction of tol by one order of magnitude roughly doubles the number of coils that contribute at the field point relative axial components greater than tol. Note that with the method used by Field the calculations of the contributions of a single coil require the same number of operations wherever the coil is located relative to the specified point.

It was mentioned earlier that tol has been preset within Field such that only coils which contribute at least 0.1 percent of the total field strength at a point are considered. This does not mean that the three direction cosines can be in error by this amount. It was found that the consideration of a coil far enough away axially from a point to contribute less than 0.1 percent of the field due to all coils changed any single direction cosine by less than 10^{-4} percent. The reason for this is that the fields due to coils far from a point are nearly perfectly axial in direction. The transverse component from a single coil far away is very small so that it adds very little to B_x and B_y . Also since the field from a distant coil is nearly axial in direction, its total contributed magnitude is almost entirely due to the axial component. Note that the axial direction cosine is B_z/B_m , and that the field of the

GSP/PH/69-7

entire displaced-coil configuration at any radius is very nearly axial. Then B_z/B_m is nearly equal to one, and adding nearly equal amounts to B_z and B_m changes the ratio very little.

Summary

Field is capable of providing to a calling program the magnitude and direction cosines of \underline{B} at any non-singular point in the magnetic field of the displaced-coil configuration. Error control is accomplished by bringing the axial component of \underline{B} to within a certain percentage of the axial strength expected in an infinite system of coils.

Appendix C

The Program Tracer

This appendix describes a program called "Tracer" which is designed to compute the paths through space of field lines in the magnetic field of the displaced-coil configuration. The appendix reiterates the objectives of the study for which Tracer is designed, and it describes the methods by which Tracer meets those objectives.

Operating instructions are provided for using Tracer. The appendix is concluded with an analysis of the control of errors of integration. Fig. 10 is a flow diagram of Tracer, and Fig. 11 is a listing of the computer code.

Objectives of Tracer

It is very useful to investigate two properties of the magnetic field of the displaced-coil configuration. First the field lines are expected to exhibit a pronounced helical twist similar to the helix on which the coil centers lie. This characteristic is called the first order twist. Also secondary rotations of the entire pattern of lines about the axis may exist.

There then is a need for a computer program to numerically integrate the paths of the magnetic field lines of the coil system. It is the objective of Tracer to integrate the paths of field lines which begin at selected coordinates in the zero plane of a parametrically

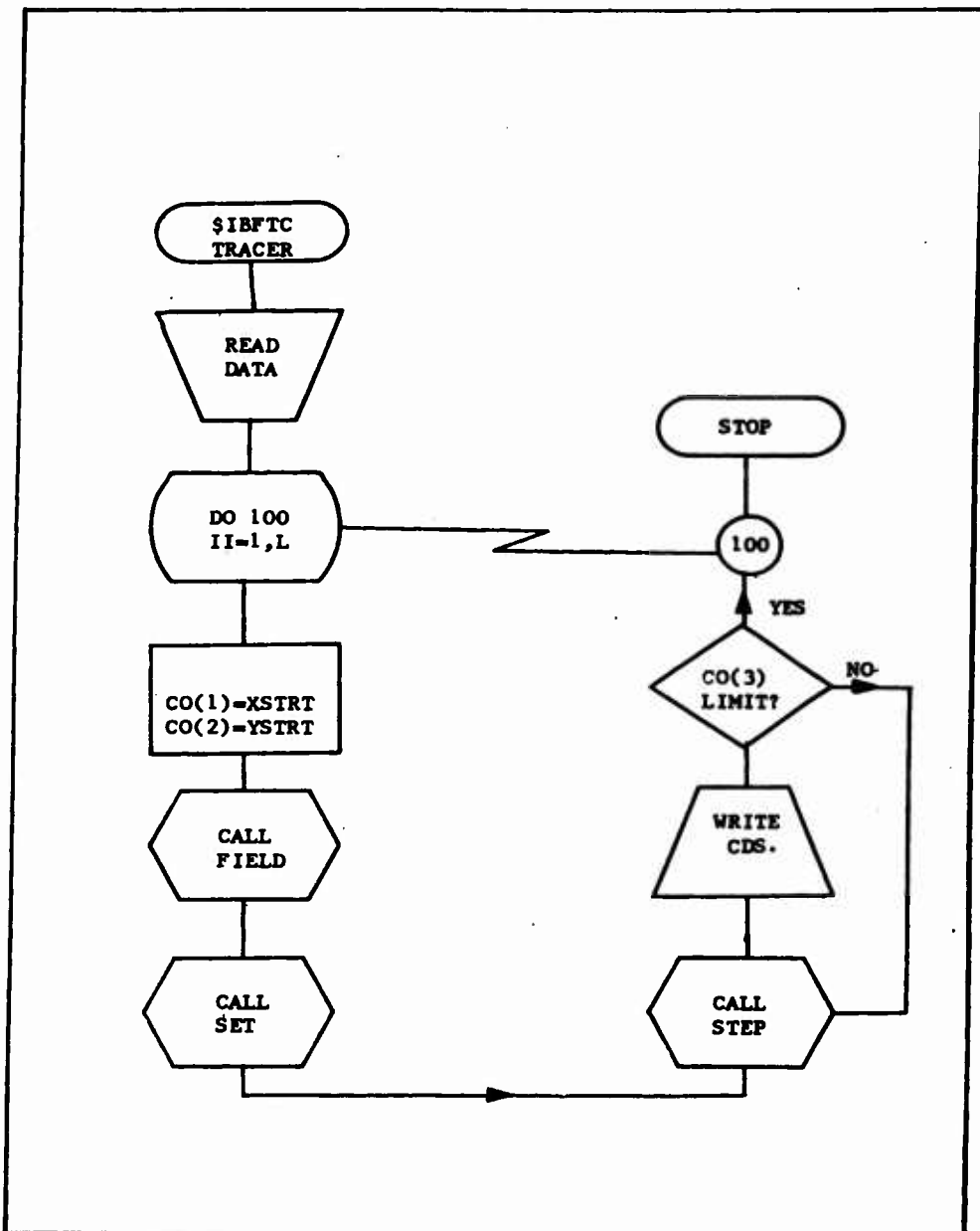


Fig. 10. Flow Diagram of Tracer

```

$IBFTC TRACER
  DIMENSION XSTRT(10),YSTRT(10),CO(3)
  EXTERNAL FUN
  LOGICAL MODE
  REAL LIMIT
  1 READ(5,81) SPACE,DISP,ALPHA,L,CN,
   1(XSTRT(I),YSTRT(I),I=1,10)
  81 FORMAT(6X,2F5.2,F5.1,I4,F5.0)
   15X,10F5.2/5X,10F5.2)
   WRITE(6,92) SPACE,DISP,ALPHA,L
  92 FORMAT(1H1,10X,19HSPACE,BE7E11,CO(2),F6.2)
   110X,27HDISPLACEMENT OF COIL CENTER,F6.2/
   210X,21HANGLE BETWEEN CENTERS,F6.1,8H DEGREES//)
   310X,15HNUMBER OF LINES,I4//)
   ALPHAR=ALPHA/57.3
   LIMIT=CN*SPACE*360./ALPHA
   DIS=.00001
   DSMIN=.05
   DSMAX=1.0
   N=3
   DO 100 II=1,L
   WRITE(6,99)
   19X,6HLENGTH,4X,4HSIZE,10X,1HX,1X,1HY,2X,1HZ//)
   S=0.
   DS=.20
   CO(1)=XSTRT(II)
   CO(2)=YSTRT(II)
   CO(3)=0.
   CALL FIELD(CO,DCO,BM,SPACE,DISP,ALPHA)
C CALL SET....INITIATES INTEGRATION
   CALL SET(N,S,CO,DS,FUN,DIS,.FALSE.,.DSMAX,DSMIN)
C A SAMPLE OUTPUT FORMAT...LENGTH, STEP SIZE, POSITION, DS
   20 WRITE(6,91)S,DS,CO(1),CO(2),CO(3)
  91 FORMAT(5X,5F10.4)
C CALL STEP....INTEGRATES EACH STEP
   CALL STEP
   21 IF(CO(3)-LIMIT) 22,44,29
  22 J=J+1
   WRITE(6,90)
  90 FORMAT(1H1)
   GO TO 20
  29 CONTINUE
 100 CONTINUE
   STOP
   END

```

Fig. 11. Listing of Tracer

Table IV

Definitions of Fortran Variables in Tracer

Fortran Name	Definitions
CN	Number of first-order cycles covered
DCO	3-matrix of direction cosines
DIS	Parameter specifying accuracy in STEP
DSMAX (DSMIN)	Maximum (minimum) size of DS
DS	Increment of independent variable
J	Number of integrating steps
L	Number of field lines to be integrated
LIMIT	Maximum axial distance of integration
MODE	Logical constant specifying variable (fixed) DS if .False. (.True.)
N	Number of differential equations (three)
S	Size of independent variable
XSTART, YSTART	X-Y coordinates of starting point of field line

adjustable coil configuration. It is intended that the user be able to control both the lengths of the lines and the maximum computational error that can arise in the coordinates of points on the lines.

Method

A magnetic field line is by definition in the same direction as the local magnetic strength vector. Field lines may be generated mathematically by successively integrating over an incremental distance the direction cosines of the local \underline{B} vector.

The Subroutine DFEQ. Tracer calls upon a subroutine called "DFEQ" written by Mr. Paul J. Nikolai of the Aerospace Research Laboratories at Wright-Patterson Air Force Base, Ohio. The subroutine is written for the Fortran IV computer language.

DFEQ is designed to integrate in a step-wise manner a set of simultaneous first-order differential equations. It requires a subroutine written by the user to supply the differentials of the dependent variables. Field is the necessary subroutine for this study. Consult Appendix B for a description of Field.

DFEQ integrates the first three steps of a series using a classical Runge-Kutta method (Ref 15:56). A four-point Adams-Bashforth-Adams-Moulton predictor-corrector scheme is applied to the fourth and succeeding points.

DFEQ can be used in a very useful mode to vary the size of the integrating increment in order to meet a

certain tolerance for accuracy. Denote by Y_i^P and Y_i^C the predicted and corrected values, respectively, of the i th dependent variable at any given point. "Dis" is a parameter specified in the program calling DFEQ. Define

$$\text{err} = \frac{\max [Y_i^C - Y_i^P]}{14 \max [1, Y_i^C]} \quad (106)$$

If err is greater than dis for any 'i' the step size currently used by DFEQ is halved, and the test is applied again over the same region. If $100 \times \text{err}$ is less than dis, the step size is doubled for succeeding integrations. Hence, DFEQ incorporates a mechanism for control of the error inherent in the approximate integration method it employs.

Dis is preset for the convenience of the user to a value which guarantees an agreement of .001 percent between the predicted and corrected values of any position coordinate. This tolerance is more than adequate to prevent cumulative error great enough to obscure the actual paths of the lines.

Operating Instructions

This section gives instructions necessary to the use of Tracer. Field must be compiled in the computer along with Tracer. The read statement in Fig. 11 relates how the data cards must be prepared. "L" is the number of lines to be integrated; up to ten lines, starting at the coordinates (XSTART,YSTART) in a zero plane, may be traced. The distance over which the lines are to be traced is specified by

selecting a multiple number (CN) of cycles of coil displacement.

Fig. 6 is an example of the output listing provided by Tracer. It is a simple tabulation of the progress of the integration for a single line.

Comments on Accuracy

The section on method explains that dis is specified within Tracer to provide for a maximum relative error per step of 10^{-5} in the coordinates of points on the field lines. On the basis of statistical random error after say N steps the relative error in any field line coordinate should be less than

$$10^{-5} \sqrt{N}$$

From studies of the average drifts of field lines over one hundred cycles of first order twist for various coil configurations it was determined that the error given above amounts to less than .001 of the average magnitude of the drifts. Since only a qualitative understanding of the slow drifts was sought, dis was not reduced to attain greater accuracy in the integration of field lines. For the study of first order field line twist a relative accuracy of 10^{-5} per step was judged more than satisfactory.

Summary

In summary, Tracer is a program which integrates the paths of field lines in the displaced-coil configuration.

GSP/PH/69-7

The method of calculation provides for the control of error. The configuration of coils, the number of lines, their lengths, and starting points are selected by the user.

Appendix D

Collision Force Between Distributions

Mention is made in Chapter III of a term which in the MHD equations can be used to account for interactions between particle distributions. The nature of this interaction is that of a drag force arising from collisions between different particles. Treated as an average the force between distributions can be found as a moment of either distribution function. Define

$$F_C = m \int_{\underline{v}} \frac{df}{dt} d\underline{v} \quad (107)$$

(Ref 16:157), where df/dt is the change due to collisions, and the integration must be over all possible values of particle velocity. This appendix deals with the evaluation of this integral.

Collision Cross Section

Define $\sigma(\underline{v} \underline{v}')$ as the geometric cross section for a change in particle velocity from \underline{v} to \underline{v}' due to an encounter with a different kind of particle. Assuming a simple Coulomb collision between the particle and another of velocity \underline{u} , the cross section in center-of-mass coordinates is

$$\sigma(\bar{q}, \theta) = \left[\frac{q q_0}{8\pi\epsilon_0 M} \right] \left[q \sin \frac{\theta}{2} \right]^{-4} \quad (108)$$

(Ref 18:150). θ is the scatter angle measured between \underline{v} and \underline{v}' , and

$$g = [\underline{u} - \underline{v}] \quad (109)$$

q and q_s are the charges of the struck and striking particles, respectively, and M is the reduced mass of the system of the two particles.

Force Per Particle

Call $f(\underline{v})$ and $F(\underline{u})$ the local distribution functions of the struck and striking particles, respectively. The flux of bombarding particles relative to a system of particles traveling at \underline{v} is then $g \cdot F(\underline{u})$. Using these definitions the probability per unit time of \underline{v} changing to \underline{v}' due to a collision is

$$P[\underline{v} \rightarrow \underline{v}'] = g F(\underline{u}) \sigma(g, \theta) \quad (110)$$

Define the change in momentum per unit time.

$$d \langle \underline{f}_c \rangle = m [\underline{v}' - \underline{v}] P(\underline{v} \rightarrow \underline{v}') \quad (111)$$

It is necessary in the integration of Eq (111) to account for all cases, represented by the possible values of \underline{v}' . Assume for a moment that \underline{v} and \underline{u} are known before a collision. The magnitude of \underline{v}' is restricted by the conservation of energy and momentum; it is in principle known from \underline{v} and \underline{u} . Consideration of all possible directions of \underline{v}' , or equivalently, all possible θ would therefore be tantamount to consideration of all \underline{v}' . We therefore

integrate over the possible scatter angles θ to evaluate $\langle \mathcal{F}_c \rangle$.

It is convenient to transform to a center-of-mass coordinate system. Define the following:

m = mass of the target particle

m_o = mass of impending particle

$\underline{v} = (m\underline{v} + m_o\underline{u})/(m + m_o)$

$M = m m_o/(m + m_o)$

Then $\langle \mathcal{F}_c \rangle$ becomes

$$\langle \mathcal{F}_c \rangle = \int m g F(\underline{u}) \left[-\frac{M}{m} \right] [\underline{g}' - \underline{g}] \sigma(g, \theta) d\theta \quad (112)$$

Define also an orthogonal, spherical polar coordinate system with \underline{g} as one of the orthogonal axes such that

$$\underline{g}' = \underline{g} \left[\hat{g} \cos \theta + \hat{\lambda} \sin \theta \cos \varphi + \hat{\alpha} \sin \theta \sin \varphi \right] \quad (113)$$

This definition merely puts $(\underline{g}' - \underline{g})$ in a more useful form.

$$[\underline{g}' - \underline{g}] = 2g \sin \frac{\theta}{2} \left[-\hat{g} \sin \frac{\theta}{2} \right. \\ \left. + \hat{\lambda} \cos \frac{\theta}{2} \cos \varphi + \hat{\alpha} \cos \frac{\theta}{2} \sin \varphi \right] \quad (114)$$

Now define $\langle F(g, \underline{v}) \rangle$ as the average force per particle due to collisions. It can be evaluated as the volume integral of $\langle \mathcal{F}_c \rangle$.

$$\langle F(g, \underline{v}) \rangle = \int d \langle \mathcal{F}_c \rangle d\Omega \quad (115)$$

where

$$d\Omega = 2 \sin \frac{\theta}{2} \cos \frac{\theta}{2} d\theta d\varphi \quad (116)$$

is the differential solid angle in a spherical coordinate system. Only the \hat{g} integral is non-zero.

$$\langle F(g, V) \rangle = \frac{\hat{g}}{4\pi Mg^2} \left[\frac{q q_0}{\epsilon_0} \right]^2 F(u) \ln \left[\sin^2 \frac{\theta}{2} \min \right] \quad (117)$$

where θ_{\min} is the scatter angle corresponding to the so-called cut-off distance for collisions. Define

$$\lambda = \sin^{-1} \frac{\theta}{2} \min \quad (118)$$

Spitzer discusses the arguments concerning the choice of the cut-off distance. His resulting equation for λ in mks units is

$$\lambda = \frac{12\pi}{q_0^2 q} \left[\frac{\epsilon_0^3 k^3 T^3}{n} \right]^{1/2} \quad (119)$$

(Ref 16:127).

Volumetric Force

Eq (117) then gives the time-averaged force per particle due to Coulomb collisions between unlike particles.

Define F_c as the volumetric average force. It can be evaluated as the moment of the target particle distribution.

$$F_c = \int f(v) F(g, V) d^3 V d^3 g \quad (120)$$

In order to calculate the components of this force in cylindrical coordinates the integral is dotted with the unit vector \hat{m} in the direction of the desired force component.

$$F_{cm} = \left[\frac{q q_0}{2\pi\epsilon_0} \right]^2 \pi \ln \Lambda \int f(v) F(u) \frac{\hat{g} \cdot \hat{m}}{g^2} dV dg \quad (121)$$

Before attempting any integrations it is use to choose v in cartesian coordinates and g in spherical coordinates. Then the respective differential volumes are

$$dV = dV_r dV_\theta dV_z \quad (122)$$

$$dg = g^2 \sin \varphi d\theta d\varphi dg \quad (123)$$

The limits on the integration of these differentials are

$$-\infty < V_r, V_\theta, V_z < +\infty$$

$$-\pi \leq \theta \leq \pi$$

$$0 \leq \varphi \leq \pi$$

$$0 \leq g < \infty$$

In cylindrical coordinates the three dot products with \hat{g} are

$$\hat{g} \cdot \hat{r} = \sin \varphi \cos \theta \quad (124)$$

$$\hat{g} \cdot \hat{\theta} = \sin \varphi \sin \theta \quad (125)$$

$$\hat{g} \cdot \hat{z} = \cos \varphi \quad (126)$$

The generalized form of the distribution functions which apply under the assumptions in force has been derived in Chapter III. The target particle distribution is given as an example.

$$f(\underline{v}) = n \left[\frac{\beta_m}{2\pi} \right]^{3/2} \exp -\frac{1}{2} \beta_m [\underline{v} + \underline{r} \times \underline{w}]^2 \quad (127)$$

Recall the definitions of the center-of-mass velocity \underline{v} and the relative velocity \underline{g} . The product $f(\underline{v})F(\underline{u})$ in terms of these is

$$f(\underline{v})F(\underline{u}) = nn_0 \left[\frac{\beta \beta_{omm}}{4\pi^2} \right]^{3/2} \exp \left[-\frac{1}{2} [\beta_m + \beta_{om_0}] \right. \\ \left. [\underline{v} - [\beta - \beta_0] M \bar{g} + [\beta_{wm} + \beta_{owm_0}] \underline{r} \hat{\theta}]^2 \right] \quad (128)$$

$$- \frac{1}{2} \frac{\beta \beta_{omm}}{[\beta_m + \beta_{om_0}]} \left[\bar{g} - [\omega_0 - \omega] \underline{r} \hat{\theta} \right]^2 \}$$

Integration of F_{cm} over the three components of \underline{v} yields a factor of

$$\left[\frac{2\pi}{\beta_m + \beta_{om_0}} \right]^{3/2}$$

(Ref 8:284).

To simplify the remaining integral in \underline{g} define the following:

$$s = g \left[\frac{\beta \beta_{omm}}{2 \beta_m + \beta_{om_0}} \right]^{1/2} \quad (129)$$

$$\rho_0 = r[\omega_0 - \omega] \left[\frac{\beta \beta_0 m m_0}{2 \beta m + \beta_0 m_0} \right]^{1/2} \quad (130)$$

Then the second exponential term in the product $f(\underline{v})F(\underline{u})$ can be rewritten.

$$\begin{aligned} & -\frac{1}{2} \left[\frac{\beta \beta_0 m m_0}{\beta m + \beta_0 m_0} \right] \left[\bar{g} - r[\omega_0 - \omega] \hat{\Theta} \right]^2 \\ & = -[\delta - 2\rho_0 \delta \sin \theta \sin \varphi + \rho_0^2] \end{aligned} \quad (131)$$

$$= -[\delta - \rho_0 \sin \theta \sin \varphi]^2 + \rho_0^2 [1 - \sin^2 \theta \sin^2 \varphi] \quad (132)$$

The integral for F_{cm} is then

$$F_{cm} = \left[\frac{q q_0}{2\pi\epsilon_0} \right]^2 \frac{\ln \Lambda}{2\pi^{3/2}} n n_0 \frac{\beta \beta_0 [m + m_0]}{\beta m + \beta_0 m_0}$$

$$\begin{aligned} & \int d\theta \int d\varphi [\hat{g} \cdot \hat{m}] \sin \varphi \int d\delta [\delta - \rho_0 \sin \theta \sin \varphi]^2 \\ & \quad + \rho_0^2 [1 - \sin^2 \theta \sin^2 \varphi] \end{aligned} \quad (133)$$

Consider separately the three integrals corresponding to the three different terms of $\hat{g} \cdot \hat{m}$. The \hat{r} and \hat{z} dot products integrate to zero by properties of odd functions of θ and φ . The $\hat{\Theta}$ component integral is

$$I_\Theta = \int d\theta \int d\varphi \sin^2 \varphi \sin \theta \quad (134)$$

$$= \int_0^\infty d\delta \exp - [\delta^2 + \rho_0^2 [1 - \sin^2 \theta \sin^2 \varphi]] \quad (135)$$

$$= \frac{2\pi}{\rho_0^2} \int_0^{\rho_0} e^{-x^2} dx - \frac{1}{\rho_0} e^{-\rho_0^2} \quad (136)$$

I_θ can be written in terms of the error function, $\bar{\Phi}$.

$$I_\theta = \frac{\pi^{3/2}}{\rho_0^2} \left[\bar{\Phi}(\rho_0) - \rho_0 \bar{\Phi}'(\rho_0) \right] \quad (137)$$

(Ref 10:696). Although $\bar{\Phi}$ is not analytic, series expansions can be used to approximate it if the argument ρ_0 is less than one.

$$\bar{\Phi}(\rho_0) = \frac{2}{\pi^{3/2}} \sum_{n=0}^{\infty} \frac{(-1)^n \rho_0^{2n+1}}{n! [2n+1]} \quad (138)$$

Therefore the complete expression for the only finite component of F_c is

$$F_c = \hat{\Theta} \left[\frac{q q_0}{\epsilon_0} \right]^2 \frac{\ln \Lambda_{nno}}{2\pi^{3/2}} \frac{BB_0 [m+m_0]}{[B_m + B_{0m_0}]} \quad (139)$$

$$\sum_{n=1}^{\infty} \frac{(-1)^{n+1} \rho_0^{2n-1}}{[2n+1] [n-1]!}$$

In summary a volumetric average force has been derived which can be used to account for the inter-distribution force arising from Coulomb collisions. This force turns out to be in the azimuthal direction only, and from the definition ρ_0 it depends on the difference between the azimuthal drift velocities of the two particle distributions.

Vita

Richard Dean Franklin [REDACTED]

[REDACTED], the son of Dewey Ray Franklin and Ellen Margaret Franklin. He was graduated from Clemson University, Clemson, South Carolina, in May, 1967, with a Bachelor of Science degree in Electrical Engineering. He was commissioned as a Second Lieutenant in the United States Air Force upon graduation from college. His first military assignment was to the Air Force Institute of Technology in the Graduate Space Physics curriculum.

Permanent address: [REDACTED]

This thesis was typed by Mrs. Shirley Tischer.

Unclassified

Security Classification

DOCUMENT CONTROL DATA - R&D

(Security classification of title, body of abstract and indexing annotation must be entered when the overall report is classified)

1. ORIGINATING ACTIVITY (Corporate author)		2a. REPORT SECURITY CLASSIFICATION	
Air Force Institute of Technology (AFIT-SE) Wright-Patterson AFB, Ohio 45433		Unclassified	
2. REPORT TITLE		2b. GROUP	
Containing Controlled Fusion Reactions With Crossed Electric and Magnetic Fields			
4. DESCRIPTIVE NOTES (Type of report and inclusive dates) AFIT Thesis			
5. AUTHOR(S) (Last name, first name, initial) FRANKLIN, Richard D. 1st Lt USAF			
6. REPORT DATE June 1969	7a. TOTAL NO. OF PAGES 106	7b. NO. OF REFS 20	
8a. CONTRACT OR GRANT NO.	8b. ORIGINATOR'S REPORT NUMBER(S) GSP/PH/69-7		
9a. PROJECT NO. c. N/A	9b. OTHER REPORT NO(S) (Any other numbers that may be assigned this report)		
10. AVAILABILITY/LIMITATION NOTES This document is subject to special export controls and each transmittal to foreign governments or foreign nationals may be made only with prior approval of the Dean of Engineering, Air Force Institute of Technology, (AFIT-SE), Wright-Patterson Air Force Base, Ohio 45433			
11. SUPPLEMENTARY NOTES	12. SPONSORING MILITARY ACTIVITY Plasma Physics Research Laboratory Aerospace Research Laboratories Wright-Patterson AFB, Ohio 45433		
13. ABSTRACT <p>A toroidal magnetic plasma containment configuration is proposed wherein coils are centered on a closed helix. It is possible to optimize the qualities of the field by adjusting the coil configuration. The equations describing an equilibrium plasma in an axisymmetric system are derived for the radial profiles of the particle density distributions, radial and azimuthal drift velocities, and the electric and magnetic field strengths necessary to maintain equilibrium.</p>			

Unclassified
Security Classification

<p>14. KEY WORDS</p> <p>Plasma Containment Toral Configuration Axisymmetric Magnetic Field Equilibrium</p>	<p>LINK A</p>	<p>LINK B</p>	<p>LINK C</p>																		
	<table border="1"> <thead> <tr> <th>ROLE</th> <th>WT</th> <th>ROLE</th> <th>WT</th> <th>ROLE</th> <th>WT</th> </tr> </thead> </table>	ROLE	WT	ROLE	WT	ROLE	WT	<table border="1"> <thead> <tr> <th>ROLE</th> <th>WT</th> <th>ROLE</th> <th>WT</th> <th>ROLE</th> <th>WT</th> </tr> </thead> </table>	ROLE	WT	ROLE	WT	ROLE	WT	<table border="1"> <thead> <tr> <th>ROLE</th> <th>WT</th> <th>ROLE</th> <th>WT</th> <th>ROLE</th> <th>WT</th> </tr> </thead> </table>	ROLE	WT	ROLE	WT	ROLE	WT
ROLE	WT	ROLE	WT	ROLE	WT																
ROLE	WT	ROLE	WT	ROLE	WT																
ROLE	WT	ROLE	WT	ROLE	WT																
INSTRUCTIONS																					
<p>1. ORIGINATING ACTIVITY: Enter the name and address of the contractor, subcontractor, grantee, Department of Defense activity or other organization (corporate author) issuing the report.</p> <p>2a. REPORT SECURITY CLASSIFICATION: Enter the overall security classification of the report. Indicate whether "Restricted Data" is included. Marking is to be in accordance with appropriate security regulations.</p> <p>2b. GROUP: Automatic downgrading is specified in DoD Directive 5200.10 and Armed Forces Industrial Manual. Enter the group number. Also, when applicable, show that optional markings have been used for Group 3 and Group 4 as authorized.</p> <p>3. REPORT TITLE: Enter the complete report title in all capital letters. Titles in all cases should be unclassified. If a meaningful title cannot be selected without classification, show title classification in all capitals in parenthesis immediately following the title.</p> <p>4. DESCRIPTIVE NOTES: If appropriate, enter the type of report, e.g., interim, progress, summary, annual, or final. Give the inclusive dates when a specific reporting period is covered.</p> <p>5. AUTHOR(S): Enter the name(s) of author(s) as shown on or in the report. Enter last name, first name, middle initial. If military, show rank and branch of service. The name of the principal author is an absolute minimum requirement.</p> <p>6. REPORT DATE: Enter the date of the report as day, month, year; or month, year. If more than one date appears on the report, use date of publication.</p> <p>7a. TOTAL NUMBER OF PAGES: The total page count should follow normal pagination procedures, i.e., enter the number of pages containing information.</p> <p>7b. NUMBER OF REFERENCES: Enter the total number of references cited in the report.</p> <p>8a. CONTRACT OR GRANT NUMBER: If appropriate, enter the applicable number of the contract or grant under which the report was written.</p> <p>8b, 8c, & 8d. PROJECT NUMBER: Enter the appropriate military department identification, such as project number, subproject number, system numbers, task number, etc.</p> <p>9a. ORIGINATOR'S REPORT NUMBER(S): Enter the official report number by which the document will be identified and controlled by the originating activity. This number must be unique to this report.</p> <p>9b. OTHER REPORT NUMBER(S): If the report has been assigned any other report numbers (either by the originator or by the sponsor), also enter this number(s).</p> <p>10. AVAILABILITY/LIMITATION NOTICES: Enter any limitations on further dissemination of the report, other than those imposed by security classification, using standard statements such as:</p> <ul style="list-style-type: none"> (1) "Qualified requesters may obtain copies of this report from DDC." (2) "Foreign announcement and dissemination of this report by DDC is not authorized." (3) "U. S. Government agencies may obtain copies of this report directly from DDC. Other qualified DDC users shall request through ." (4) "U. S. military agencies may obtain copies of this report directly from DDC. Other qualified users shall request through ." (5) "All distribution of this report is controlled. Qualified DDC users shall request through ." <p>If the report has been furnished to the Office of Technical Services, Department of Commerce, for sale to the public, indicate this fact and enter the price, if known.</p> <p>11. SUPPLEMENTARY NOTES: Use for additional explanatory notes.</p> <p>12. SPONSORING MILITARY ACTIVITY: Enter the name of the departmental project office or laboratory sponsoring (paying for) the research and development. Include address.</p> <p>13. ABSTRACT: Enter an abstract giving a brief and factual summary of the document indicative of the report, even though it may also appear elsewhere in the body of the technical report. If additional space is required, a continuation sheet shall be attached.</p> <p>It is highly desirable that the abstract of classified reports be unclassified. Each paragraph of the abstract shall end with an indication of the military security classification of the information in the paragraph, represented as (TS), (S), (C), or (U).</p> <p>There is no limitation on the length of the abstract. However, the suggested length is from 150 to 225 words.</p> <p>14. KEY WORDS: Key words are technically meaningful terms or short phrases that characterize a report and may be used as index entries for cataloging the report. Key words must be selected so that no security classification is required. Identifiers, such as equipment model designation, trade name, military project code name, geographic location, may be used as key words but will be followed by an indication of technical context. The assignment of links, rules, and weights is optional.</p>																					